

Optical and Infrared Photometry of the Type Ia Supernovae 1999da, 1999dk, 1999gp, 2000bk, and 2000ce

Kevin Krisciunas¹, Mark M. Phillips², Christopher Stubbs³, Armin Rest³, Gajus Miknaitis³, Adam G. Riess⁴, Nicholas B. Suntzeff¹, Miguel Roth², S. E. Persson⁵, and
Wendy L. Freedman⁵

¹Cerro Tololo Inter-American Observatory, Casilla 603, La Serena, Chile

²Las Campanas Observatory, Carnegie Observatories, Casilla 601, La Serena, Chile

³Department of Astronomy, University of Washington, Box 351580, Seattle, WA
98195–1580

⁴Space Telescope Science Institute, 3700 San Martin Drive, Baltimore, MD 21218

⁵Observatories of the Carnegie Institution of Washington, 813 Santa Barbara Street,
Pasadena, CA 91101

Electronic mail: kkrisciunas, nsuntzeff@noao.edu

mmp, miguel@lco.cl

stubbs, rest, gm@astro.washington.edu

ariess@stsci.edu

persson, wendy@ociw.edu

Received _____; accepted _____

ABSTRACT

We present BVRI photometry of the Type Ia supernovae 1999da, 1999dk, 1999gp, 2000bk, and 2000ce, plus infrared photometry of three of these. These objects exhibit the full range of decline rates of Type Ia supernovae. Combined optical and infrared data show that families of V – infrared color curves can be used to derive the host extinction (A_V) of these objects. Existing data do not yet allow us to construct these loci for all color indices and supernova decline rates, but the V–K color evolution is sufficiently uniform that it allows the determination of host extinction over a wide range of supernova decline rates to an accuracy of roughly ± 0.1 mag. We introduce a new empirical parameter, the mean I-band flux 20 to 40 days after maximum light, and show how it is directly related to the decline rate.

Subject headings: supernovae, photometry

1. Introduction

Over the past decade Type Ia supernovae (SNe) have been shown to be excellent standardizable candles (Leibundgut 2000, and references therein). The most popular models rely on the detonation (or deflagration) of a C-O white dwarf at the Chandrasekhar mass. Because the amount of fuel in the explosion is approximately the same, the resulting explosion has about the same amount of energy. The optical light curve is powered by the amount of ^{56}Ni that is produced, typically $0.6 M_{\odot}$ (Nomoto, Iwamoto, & Kishimoto 1997).

However, it is known that Type Ia SNe *do* exhibit a range of peak luminosities, and models bear out that the least luminous examples, such as SN 1991bg, produce only $\approx 0.1 M_{\odot}$ of ^{56}Ni , while the more luminous examples, such as SN 1991T, produce $\approx 1.1 M_{\odot}$ (Cappellaro et al. 1997; Contardo, Leibundgut, & Vacca 2000). Details of modeling the physics of the explosion, along with a comparison with the well observed SNe 1991T and 1992A can be found in Pinto & Eastman (2000a, 2000b); see also Höflich, Khokhlov, & Wheeler (1995).

It is now well known that the luminosities of Type Ia SNe obey a decline rate relation (Phillips 1993, Phillips et al. 1999). Hamuy et al. (1996a, 1996b) and Phillips et al. (1999) have developed a three filter (BVI) template-fitting procedure, commonly referred to as the “ $\Delta m_{15}(\text{B})$ method”, for deriving distances to Type Ia SNe and for estimating the host galaxy dust reddening. Here $\Delta m_{15}(\text{B})$ is the number of B-band magnitudes the SN dims in the first 15 days after the time of maximum light. Those with slower decline rates are intrinsically brighter at maximum light. It is important to note that slow decliners are slow risers; also, fast risers are fast decliners.¹

¹The correlation of rise rate with decline rate is well known to supernova observers, but one rarely finds the idea expressed this simply. The template *stretch method* of Perlmutter

Riess, Press, & Kirshner (1996, hereafter RPK) and Riess et al. (1998a) developed the multi-color light curve shape (MLCS) method of fitting the BVRI photometry of Type Ia SNe. The key parameter, called Δ , is the number of V-band magnitudes (at maximum) that a Type Ia SN is brighter than ($\Delta < 0$) or fainter than ($\Delta > 0$) some fiducial object. From the calibration of the distances of the host galaxies using different methods, a Type Ia SN with $\Delta = 0.00$ has a corresponding absolute magnitude at maximum of $M_V = -19.46$. The range of Δ (see RPK) is roughly -0.56 (for SN 1991T) to $+1.44$ mag (for SN 1991bg).

It is worth emphasizing that both the $\Delta_{m_{15}(B)}$ method and MLCS use photometry from multiple filters to derive a single parameter keyed to a specific filter. The main difference is that MLCS uses a linear interpolation method to derive a *continuum* of templates, while the $\Delta_{m_{15}(B)}$ method uses a *finite number* of templates derived from fits to the data of specific, individual SNe.

Recently, Krisciunas et al. (2000, hereafter Paper I) showed that Type Ia SNe which are spectroscopically “normal” and which have $-0.38 \lesssim \Delta \lesssim +0.23$ mag exhibit uniform V – near infrared color curves. We found that V–K colors get linearly bluer from 9 days before B-band maximum until 6 days after $T(B_{max})$, after which they redden linearly, until roughly 27 days after $T(B_{max})$. V–H colors obey quite similar color evolution. However, V–J colors exhibit considerably more scatter for objects with comparable reddening; given

et al. (1997) uses templates running from *negative* 10 days to +80 days with respect to the time of B-band maximum. By definition, the B-band light is on the rise for $t < 0$, since $t = 0$ is the time of B_{max} . The method of Riess, Press, & Kirshner (1996), which generates templates from $t = -10$ to +90 days with respect $T(B_{max})$, and that of Phillips et al. (1999) speak of the *width* of the light curves being larger for the slowly declining Type Ia SNe. All three methods imply that slow risers are slow decliners, and fast risers are fast decliners. Recently, this has been shown to be quantitatively true by Goldhaber et al. (2001).

the complexity of the spectrum of Type Ia SNe in the J-band (see Wheeler et al. 1998), it is not surprising that any color index involving J would behave differently from object to object.

Paper I showed that there exist fiducial color loci which can be used to determine the total absorption (A_V) towards Type Ia SNe, even if the reddening in the host galaxy is significantly different than the reddening by dust in our Galaxy. For example, SN 1999cl in the Virgo Cluster galaxy M 88 was reddened, with $R_V \equiv A_V/E(B-V) \approx 1.8$, vastly different than the canonical value of 3.1 (Snedden et al. 1978; Rieke & Lebofsky 1985).

Because less than 100 Type Ia SNe have well characterized BVRI light curves, and only a small percentage were observed in the near infrared (see Meikle 2000 for a summary of the infrared observations), we have been carrying out a program of such observations of newly discovered objects. In this paper we provide optical light curves of SNe 1999da, 1999dk, 1999gp, 2000bk, and 2000ce. The last three were also measured in the near infrared. In addition to providing finding charts, field star sequences, and supernova photometry, we also introduce a new parameter which is well correlated with the intrinsic brightness of these objects.

2. Observations

SN 1999da was discovered by Johnson & Li (1999) from images of 2.4 and 5.4 July 1999 UT. It occurred in NGC 6411, which Skiff (private communication) indicates is best classified as a mid-stage lenticular galaxy of type SA0⁻. Spectra by Filippenko (1999) and Jha et al. (1999a) indicated that this would be a subluminous Type Ia SN similar to SNe 1991bg (Leibundgut et al. 1993) and 1998de (Modjaz et al. 2001).

SN 1999dk was discovered by Modjaz & Li (1999) from images of 12.5 and 13.5 August

1999 UT. It occurred in the Sc galaxy UGC 1087.

SN 1999gp was discovered in the Sb galaxy UGC 1993 by Papenkova & Li (1999) on 23.2 December 1999 UT. A spectrum taken on 2.2 January 2000 UT and reported by Jha et al. (1999b) indicated, from the absence of a strong Si II 580 nm feature, that this SN would prove to be overluminous. Nevertheless, in this same spectrum, which was obtained ~ 5 days before B-band maximum, reasonably strong Si II 635.5 nm absorption is clearly present, so this SN would not appear to be as extreme as a 1991T or 1999aa-like event.

SN 2000bk was discovered in the SA0⁻ galaxy NGC 4520 by Armstrong (2000) on 12.0 April 2000.

SN 2000ce was discovered in the SBb galaxy UGC 4195 by Puckett (2000) on 8.1 May UT.

On the basis of observations of Landolt (1992) standards on photometric nights, we determined the V magnitudes and optical colors of field stars near each supernova. In the course of our calibrations we discovered that Landolt’s published value of the the V–I color of the star PG0231+051 has a systematic error. The correct value is -0.350 ± 0.017 . Stetson (private communication) confirms this; his value is -0.346 ± 0.018 . Without taking this into account, our derived V–I colors for SN 1999gp would be in error by up to 0.1 mag.

All of our photometry of SN 1999gp and 2000ce was obtained with the Apache Point Observatory (APO) 3.5-m telescope. All of the SN 1999dk data were taken with the University of Washington’s Manastash Ridge Observatory (MRO) 0.76-m telescope. SN 1999da was observed with both APO and MRO. SN 2000bk was observed at APO (BVRIJH photometry) and with the Las Campanas Observatory 1-m and 2.5-m telescopes (J and H).

In Figs. 1 through 5 we give finding charts for each SN. Tables 1 through 5 give coordinates of each SN, coordinates of the field stars, and optical photometry of these field

stars. The field star photometry is based on averages of four to six photometric nights of calibration per field. Differential photometry amongst the field stars for each supernova indicates no obvious variables. We find these stars to be constant at the ± 0.03 mag level or better, so differential photometry of the SNe with respect to these stars gives us confidence that any variability is attributable to the SNe themselves.

Ideally, a supernova occurs at a large enough angular distance from the luminous regions of its host galaxy and also from the field stars in our Galaxy, such that simple aperture photometry is accurate. If the supernova is superimposed on the light of the host galaxy, aperture photometry is still sufficiently accurate if the underlying light of the galaxy is reasonably uniformly distributed. This can be judged by first considering the instrumental magnitudes as a function of aperture size for the isolated field stars and comparing them to the instrumental magnitudes as a function of aperture for the supernova. If both sets of numbers converge at the same rate, then we can likely trust the aperture photometry of the SN. This is certainly the case for SNe 1999da and 2000bk, which occurred in the low-luminosity outer reaches of two early type galaxies. Aperture photometry also is justifiable in the cases of SNe 1999dk and 2000ce. However, it was clear that SN 1999gp would require reduction via image subtraction, using templates obtained after the SN had faded sufficiently. For image subtraction we used the algorithms and software of Alard & Lupton (1998), with additional scripts and improvements written by Andrew Becker and by us.

Our IR templates for SN 1999gp were obtained on 17 October 2000 and our BVRI templates were obtained on 27 November 2000, some 284 and 325 days, respectively, after the date of B-band maximum. We compared results from aperture photometry and image subtraction techniques.² The non-uniform nature of the underlying galaxy light is clearly a

²The B-band photometry required corrections of 0.01 to 0.12 mag, while the I-band

problem with this object. Image subtraction was required at all wavelengths.

Our local infrared standards for SN 2000bk were calibrated on seven photometric nights using the standard star system of Persson et al. (1998).³ The local standards for SN 2000ce were calibrated on five photometric nights using the list of Hunt et al. (1998). Local infrared standards for SN 1999gp were also calibrated with observations of standards of Hunt et al. (1998); the near infrared magnitudes of these stars were found to agree within the errors with preliminary values from the 2MASS survey (see Table 11).

For the infrared photometry of SNe 2000bk and 2000ce we compared the results of aperture photometry and PSF (point spread function) magnitudes obtained with DAOPHOT (Stetson 1987, 1990). This also involved the use of additional numerical tools developed by one of us (NBS). The PSF magnitudes typically gave smoother light curves and color curves, so we have adopted the PSF magnitudes for the infrared photometry of these two objects.

In Tables 6 through 10 we give BVRI photometry of our five SNe, based on our calibration of the local secondary “standards”. The BVRI photometry is weighted by the photon statistics of the raw data and the uncertainties resulting from the calibration of the local secondary standards. In our experience, formal uncertainties smaller than ± 0.010

photometry required corrections of 0.03 to 0.43 mag.

³The Las Campanas Observatory data were obtained with a standard H-band filter, but their J_s (“J-short”) filter has a narrower bandwidth and a different central wavelength than the more standard J filter used at Apache Point Observatory. We do not have the necessary observations of *stars* to give transformations between these infrared systems, and even if we did, the question remains as to the proper transformations required for the reduction of the *supernova* data.

mag are not to be taken too literally.

Light curves are shown in Figs. 6 through 10. On the left hand sides of Figs. 7 through 10 we show the MLCS fits to the BVRI data. On the right hand sides we show the BVI templates derived via the $\Delta m_{15}(B)$ method. In the case of SN 2000ce the latter method finds that two templates (1991T and 1992bc) fit the data equally well. This leads to greater uncertainty than usual regarding the time of B-band maximum, and the magnitudes at maximum. This is an inherent problem if observations of a supernova are not made closer to the time of maximum light.

We remind the reader that the MLCS method recognizes that there is inherent scatter of the V-band magnitudes and B–V, V–R, and V–I colors of supernovae *even if the photometry can be characterized by the same value of Δ* . Note the width of the “grey snakes” in Fig. 3 of RPK. MLCS solutions preferentially give greater weight to the photometry obtained at maximum light. Deviations of the templates from the photometry of an *individual* supernova is more a recognition of the inherent scatter amongst objects than a failure of the MLCS method.

Table 11 gives infrared magnitudes of local field stars. Table 12 gives near infrared photometry of SNe 1999gp, 2000bk and 2000ce.

We note in passing that we applied color terms, derived from observations of Landolt (1992) standards, to the BVRI data for the SNe, but no color terms were applied to the infrared photometry. Most of the infrared observations of SN 2000bk were obtained with the Las Campanas 1-m telescope. It was on this very telescope that the infrared standard system of Persson et al. (1998) was defined, so the color terms would be non-zero only if the optical coatings had greatly changed over time.

3. Discussion

3.1. General comments

In Table 13 we summarize various observational parameters for these five SNe based on MLCS. For comparison, in Table 14 we give light curve parameters (time of B-band maximum, decline rate, best fit magnitudes at maximum light, host reddening, and distance modulus) based on analysis similar to that of Phillips et al. (1999).

The second version of MLCS (Riess et al. 1998a) was limited to $-0.5 \leq \Delta \leq +0.5$. SN 1999da is a faster decliner than a Type Ia SN characterized by $\Delta = +0.50$, so it cannot be fit with the latest MLCS vectors. The decline rate $\Delta_{m_{15}}(B) = 1.94 \pm 0.10$ is amongst the most rapid known. Very few fast declining Type Ia SNe like 1991bg (Leibundgut et al. 1993) and 1998de (Modjaz et al. 2001) have well sampled light curves. Given the rarity of such objects and the fact that we began observing SN 1999da before maximum light, our results will eventually be valuable for the calibration of light curve fitting schemes for the low luminosity range of Type Ia SNe.

SN 1999gp showed an extremely prominent secondary maximum in the I-band, which is indicative of an overluminous Type Ia SN. For this object MLCS gives $\Delta = -0.45 \pm 0.10$ mag.

SN 2000bk was somewhat underluminous, with $\Delta = +0.43 \pm 0.15$ mag. As one can see in Fig. 9, it had a reasonably weak I-band secondary maximum, but a very strong one in the J-band.

SN 2000ce was a moderately luminous SN, with $\Delta = -0.26 \pm 0.17$ mag.

The earliest spectra obtained of SNe 1999aa, 1999da, and 1999gp predicted that the first and last were overluminous Type Ia SNe, while SN 1999da was underluminous.

Subsequent photometry proved that their light curves were very much as predicted. This underscores the insights of Nugent et al. (1995) and Riess et al. (1998b), who suggested that a spectrum taken within a week of maximum light and photometry obtained on a small number of nights near maximum make it possible to estimate the intrinsic brightness of a Type Ia SN. The results of Paper I also indicate, if such an object is spectroscopically “normal”, that H-band or K-band photometry earlier than a month after maximum light, combined with a V-band light curve, can give us the extinction (A_V) to ± 0.1 mag or better. Future supernova observing campaigns should certainly take this into account.

In Fig. 11 we show the reddening-corrected absolute magnitudes in BVI of SNe 1999da, 1999dk, 1999gp, 2000bk, and 2000ce plotted versus $\Delta m_{15}(B)$. The fainter crosses correspond to the 41 SNe in Phillips et al. (1999) with $0.01 < z < 0.1$. To these has been added the fast-declining SN 1998de (Modjaz et al. 2001). The distance to each SN was calculated from the redshift of the host galaxy (in the cosmic microwave background frame) and an assumed value of the Hubble constant of $H_0 = 65 \text{ km s}^{-1} \text{ Mpc}^{-1}$. Following Hamuy et al. (1996a), a peculiar velocity term of 600 km s^{-1} has been included in the error bars of the absolute magnitudes. The host galaxy reddening for each SN was calculated using the methods given in Phillips et al. (1999). Note that the five SNe from the present paper are in excellent agreement with the larger sample.

We note that the distance moduli for SNe 1999dk, 1999gp, 2000bk, and 2000ce are, on average, 0.22 mag larger using MLCS compared to the results based on analysis in the style of Phillips et al. (1999). For these four objects, this means that MLCS-derived distances are 11 percent larger and would lead to correspondingly smaller estimates of the Hubble constant.

3.2. Extinction and reddening

The simplest way to test the “uniformity” of our $V -$ near infrared color relations given in Paper I is to plot the $V -$ IR colors of other SNe and derive color excesses from a simple upward translation of the unreddened loci. If the color excesses from $V-J$, $V-H$, and $V-K$ imply the same value of A_V , then all is well.⁴ If there are residuals which correlate with a luminosity-related parameter (i.e. MLCS Δ or $\Delta_{m_{15}}(B)$), that is evidence that there are families of loci analogous to BVRI templates for optical photometry.

In Figs. 12, 13, and 14 we plot $V -$ IR colors for SNe 1999gp, 2000bk, and 2000ce. We also plot our unreddened loci from Paper I, along with those loci offset by various amounts.

While the $V-K$ colors of SN 1999gp are too uncertain to say anything of substance, the $V-J$ and $V-H$ colors confirm what we showed in Fig. 12 of Paper I, that in the lower right region of the diagrams the $V -$ near IR colors of unreddened, overluminous, slowly declining Type Ia SNe are to be found below the unreddened loci determined by mid-range decliners.

Given the generally low dust content of early-type galaxies and the location of SN 2000bk in the outskirts of its host, one might expect absorption by dust in its host to be minimal. MLCS gives $A_V = 0.28 \pm 0.20$ along the line of sight towards this SN. The Schlegel et al. (1998) reddening maps of our Galaxy indicate that along the line of sight to SN 2000bk the Galactic reddening is $E(B-V) = 0.025$ mag, so 0.08 mag of A_V is due to dust in our Galaxy. Analysis similar to that of Phillips et al. (1999) indicates a host reddening of $E(B-V) = 0.10 \pm 0.04$. Assuming $R_V = 3.1$ for dust in our Galaxy and the host of SN 2000bk, $A_V = 0.39 \pm 0.12$ mag. Thus, the extinction suffered by this SN would

⁴As in Paper I, we adopt the reddening calibration of Rieke & Lebofsky (1985), which gives $A_V = 1.393 E(V-J) = 1.212 E(V-H) = 1.126 E(V-K)$.

appear to be small, but not zero.

The *shape* of the V–J color curve of SN 2000bk clearly does not correspond to a simple upward translation of the unreddened locus. Even if we restrict the fit to data earlier than 18 days after B-band maximum, the implied color excess is $E(V-J) = 0.62 \pm 0.03$ mag. Using a standard dust model (Eqs. 5, 6, and 7 of Paper I) implies $A_V = 0.87 \pm 0.08$ mag, clearly much larger than the values of 0.28 ± 0.20 and 0.39 ± 0.12 quoted above. The V–H colors of SN 2000bk imply $A_V = 0.54 \pm 0.04$ mag, which is also larger than the values based on BVRI data. However, the *slope* of the V–H color curve (0.0851 ± 0.0059 mag d^{-1}) is, within the errors, identical to that of our unreddened locus (0.0840 ± 0.0042).

If we assume that the color evolution of SN 2000ce is similar to the SNe studied in Paper I, the V–J, V–H and V–K data give estimates of A_V of 1.80 ± 0.44 , 1.33 ± 0.13 , and 1.65 ± 0.12 mag, respectively, where we have included the contribution of the uncertainty of the time of B-band maximum to the error bars. *However*, the few V–J points only fit the template if we shift the data 3.0 days to the left in Fig. 12 (i.e. adopt $T(B_{max})$ 3 days later than the value given by MLCS). There is evidence (see below and Fig. 15) that we should use a bluer V–H template for this object than that of Paper I. A_V derived from V–K photometry is in excellent agreement with the value of $A_V = 1.67 \pm 0.20$ given by MLCS. This is to say that the photometry of SN 2000ce points to: 1) an ongoing suspicion that V–J is not a “well behaved” color index; 2) our V–H template from Paper I is not applicable to as wide a range of Δ as we previously thought; 3) the analysis confirms that A_V for a reddened Type Ia SN can be determine from V–K colors with an uncertainty of roughly ± 0.1 mag. In the case of SN 2000ce the uncertainty of $T(B_{max})$ contributes as much to the error budget as the photometric errors or the uncertainty of the ratio of total to selective absorption [$R_{\lambda_1} = A_{\lambda_1}/E(\lambda_1 - \lambda_2)$].

Since one of our goals is to be able to use optical and infrared data to determine values

of A_V (and hence the distances) of Type Ia SNe over the full range of decline rates, but a sufficient number of well sampled IR light curves does not yet exist, we proceed tentatively as follows. SN 1998bu data shown in Paper I and preliminary SN 1999ac data (Phillips et al., in preparation) show that the local minimum in the V–H and V–K colors a week after $T(B_{max})$ has a more gradual change of slope than the two-straight-line loci used in Paper I. We remind the reader that these loci are based on 4 supernovae unreddened in their hosts, two with minimal reddening, and two with significant reddening. If we fit fourth order curves to the “compacted” data shown in Fig. 10 of Paper I and subtract the derived color excesses $E(V-J)$, $E(V-H)$, and $E(V-K)$ of SN 1998bu (Table 10 of Paper I) from the data, we would expect the deviations of the dereddened SN 1998bu data from these new loci to be very nearly zero, and in fact they are. The mean deviations are -0.025 ± 0.031 , $+0.013 \pm 0.020$ and $+0.007 \pm 0.019$ mag, respectively, for V–J, V–H and V–K. We can then use the BVRI photometry and assumed values of IR to V-band extinction to deredden the V–J, V–H and V–K data of SNe 1999aa, 1999ac, 1999gp, 2000bk, 2000ce.⁵

In Fig. 15 we show the mean deviations from the fourth order unreddened loci of the dereddened V – near IR colors of six supernovae. Graphically, this confirms our principal finding from Paper I, in particular, that V–K colors of Type Ia SNe over a rather wide range of Δ can be fitted by the same locus, adjusted only by the V–K color excess of the object. SN 2000bk and the peculiar SN 1986G (see Fig. 12 of Paper I) show that fast decliners are intrinsically redder in V – near IR colors than mid-range decliners. SNe 1999aa and 1999gp show that slow decliners are intrinsically bluer than the mid-range decliners. The different values of A_V for SN 2000ce derived from V–H and V–K data can be explained by the fact that at $\Delta = -0.26$ we need a bluer unreddened locus for V–H

⁵We have restricted the data of SNe 1999aa, 1999ac, 1999gp, 2000bk, and 2000ce to $0 \leq t \leq 27$ days after the time of B-band maximum.

(and/or one with a different slope from 9 to 27 days after $T(B_{max})$) than the one that is our present reference.

The data of the present paper are consistent with the prediction of Paper I, namely that fast decliners, mid-range decliners, and slow decliners require families of curves to delineate their color evolution. Still, the $V - \text{near IR}$ colors of mid-range decliners may be characterized by thin enough “grey snakes” (see RPK, Fig. 3) that they can be used as an excellent basis for determining A_V .

3.3. The secondary hump in the red

One of the most characteristic features of the light curves of Type Ia SNe is the secondary maximum in the far red and near infrared (IJHK bands). Elias et al. (1981, 1985) first showed this for the JHK bands. For the I-band it was first discussed by Ford et al. (1993), and in 1993 at the Xian, China, meeting on supernovae (Suntzeff 1996). Subsequently, Hamuy et al. (1996d) provided evidence that the I-band secondary maximum is stronger and occurs later for the slowly declining Type Ia SNe. In a parallel study, RPK also showed graphically that the secondary I-band maximum is very strong for the most luminous Type Ia SNe, while there is no secondary maximum for the least luminous ones. Höflich, Khokhlov, & Wheeler (1995) explain this as a temperature/radius effect. To a first approximation, the infrared luminosity is proportional to the area of the expanding fireball, the effective temperature, and a dilution factor for scattering dominated atmospheres. If the photospheric radius (R_{ph}) is still increasing after maximum, a secondary maximum occurs due to the R_{ph}^2 term. For the subluminous examples the secondary maximum is not seen because it merges with the primary maximum. For additional discussion and references see §3.1 of Riess et al. (2000) and §4.1 of Pinto & Eastman (2000b).

We pose the question: to what extent is the luminosity at maximum of a Type Ia SN correlated with the strength of the secondary I-band maximum? For this we need well sampled I-band light curves. In Fig. 16 we show the I-band photometry of SN 1999aa from Paper I, with the I magnitudes converted to flux with respect to the I-band maximum. We have fitted a higher order polynomial to the data and determined the mean flux (based on an *integration* of the polynomial) from 20 to 40 days after the time of B-band maximum. In this example $\langle I \rangle_{20-40} = 0.617$. For a well sampled light curve and typical photometric uncertainties, this parameter should be accurate to ± 0.03 or better. In fact, two independent sets of data for SN 1996X (Riess et al. 1999; R. Covarrubias et al., unpublished) give values of $\langle I \rangle_{20-40} = 0.516$ and 0.471 , respectively, indicating an uncertainty of ± 0.023 for the mean. A third data set for SN 1996X (Salvo et al. 2001) gives $\langle I \rangle_{20-40} = 0.521$, but their I-band photometry is particularly ragged at the time of the secondary I-band maximum.

In Fig. 17 we show $\langle I \rangle_{20-40}$ vs. $\Delta m_{15}(B)$ for 23 SNe. We include four SNe from the RPK training set: 1990N and 1991T (Lira et al. 1998), 1991bg (Leibundgut et al. 1993), plus 1992A (Suntzeff et al., unpublished). SN 1992K (Hamuy et al. 1994) was a subluminous, rapid decliner. We include five other SNe from the Calán/Tololo survey (Hamuy et al. 1996c): 1992al, 1992bc, 1992bo, 1993H, and 1993O; seven of the 22 SNe from Riess et al. (1999): 1994M, 1994ae, 1995D, 1995E, 1995ac, 1995al, and 1996X; SN 1998bu (Jha et al. 1999c); SN 1999aa (Paper I); plus four of the five SNe presented in this paper. SN 2000ce was not observed early enough to get an accurate estimate of the I-band maximum. These 23 SNe have a median total color excess (i.e. sum of Galactic and host galaxy contributions) of $E(B-V) = 0.104$ mag, with only SNe 1995E and 1998bu having values greater than 0.2.

Except for SNe 1992bc and 1994M, the points plotted in Fig. 17 form a tight relation.

In the top panel of Fig. 18 we show the BVI light curves of SNe 1994ae and 1992bc. These objects have essentially identical decline rates in B and V, but SN 1992bc has a considerably weaker I-band secondary maximum. In the bottom panel of Fig. 18 we similarly show SNe 1992A and 1994M, where the latter shows a much stronger I-band maximum.

Since the SN 1992bc data were obtained with CTIO telescopes and detectors and reduced in the same manner as the data for the 10 other SNe plotted in Fig. 17 observed at CTIO, there is no reason to suspect I-band calibration problems to be the cause of its anomalous I-band secondary maximum. Similarly, SN 1994M was observed with the same equipment and reduced in the same manner as the 7 other SNe with Center for Astrophysics (CfA) data plotted in Fig. 17. The excellent agreement of the $\langle I \rangle_{20-40}$ values calculated from the CfA and CTIO data sets for SN 1996X further demonstrates that these outliers are real. Pinto & Eastman (2000b, §4.1) suggest that the details of the secondary maximum tell us something about the ignition conditions of the explosion, in particular the neutron-rich isotopes that make up the non-radioactive core.

The solid curve in Fig. 17 is a third order polynomial fit. If we eliminate SNe 1992bc and 1994M from the fit, the RMS residual is only ± 0.093 in $\Delta m_{15}(B)$. Figs. 17 and 18 show that the luminosity at maximum is directly related to the strength of the I-band secondary maximum, but that there are clearly exceptions to the rule.

The $\langle I \rangle_{20-40}$ relationship and the demonstrated usefulness of the V–H and V–K color curves for determining A_V should provide ample motivation for the gathering of optical and infrared data for Type Ia SNe.

4. Conclusions

We have presented optical photometry of SNe 1999da, 1999dk, 1999gp, 2000bk, and 2000ce. We obtained reasonably well-sampled J-band and H-band light curves of SN 2000bk, along with a small amount of infrared photometry of SNe 1999gp and 2000ce.

A combination of V-band and infrared photometry allows one to determine the extinction suffered by Type Ia SNe in their hosts. At present, however, the data only exist to do this for Type Ia SNe in the mid-range of decline rates.

By introducing a new empirical parameter, $\langle I \rangle_{20-40}$, we provide a useful way of parameterizing the strength of the I-band secondary maximum of Type Ia SNe. This is directly related to the decline rate, and hence, to the intrinsic brightness of these objects.

This paper is based in part on observations obtained with the Apache Point Observatory 3.5-meter telescope, which is owned and operated by the Astrophysical Research Consortium. IRAF is a product of the National Optical Astronomy Observatories, which is operated by the Association of Universities for Research in Astronomy, Inc., under cooperative agreement with the National Science Foundation.

We thank Eugene Magnier and Alan Diercks for the use of their infrared data reduction software. Andrew Becker provided scripts for an image subtraction pipeline. Brian Skiff kindly determined the coordinates of the field stars in Table 1 through 5. We thank Russet McMillan and Camron Hastings for observing support. We also made use of Simbad, a database of the Centre de Données astronomiques de Strasbourg.

This work was supported by NSF grant AST-9512594. C. Stubbs also acknowledges the generous support of the McDonnell Foundation.

REFERENCES

- Alard, C., & Lupton, R. H. 1998, *ApJ*, 503, 325
- Armstrong, M. 2000, IAUC No. 7402
- Cappellaro, E., Mazzali, P. A., Benetti, S., Danziger, I. J., Turatto, M., Della Valle, M., & Patat, F. 1997, *A&A*, 328, 203
- Contardo, G., Leibundgut, B., & Vacca, W. D. 2000, *A&A*, 359, 876
- Elias, J. H., Frogel, J. A., Hackwell, J. A., & Persson, S. E. 1981, *ApJ*, 251, L13
- Elias, J. H., Matthews, G., Neugebauer, G., & Persson, S. E. 1985, *ApJ*, 296, 379
- Filippenko, A. V. 1999, IAUC No. 7219
- Ford, C. H., Herbst, W., Richmond, M. W., Baker, M. L., Filippenko, A. V., Treffers, R. R., Paik, Y., & Benson, P. J. 1993, *AJ*, 106, 1101
- Freedman, W. L., Madore, B. M., Gibson, B. K., et al. 2000, *astro-ph/0012376*
- Goldhaber, G., Groom D. E., Kim, A., et al. 2001, *astro-ph/0104382*
- Hamuy, M., Phillips, M. M., Maza, J., et al. 1994, *AJ*, 108, 2226
- Hamuy, M., Phillips, M. M., Schommer, R. A., Suntzeff, N. B., Maza, J., & Avilés, R. 1996a, *AJ*, 112, 2391
- Hamuy, M., Phillips, M. M., Suntzeff, N. B., Schommer, R. A., Maza, J., & Avilés, R. 1996b, *AJ*, 112, 2398
- Hamuy, M., Phillips, M. M., Suntzeff, N. B., et al. 1996c, *AJ*, 112, 2408
- Hamuy, M., Phillips, M. M., Suntzeff, N. B., Schommer, R. A., Maza, J., Smith, R. C., Lira, P., & Avilés, R. 1996d, *AJ*, 112, 2438
- Höflich, P., Khokhlov, A. M., & Wheeler, J. C. 1995, *ApJ*, 444, 831

- Hunt, L. K., Mannucci, F., Testi, L., Migliorini, S., Stanga, R. M., Baffa, C., Lisi, F., & Vanzi, L. 1998, *AJ*, 115, 2594
- Jha, S., et al. 1999a, IAUC No. 7219
- Jha, S., et al. 1999b, IAUC No. 7341
- Jha, S., Garnavich, P., Kirshner, R. P., et al. 1999c, *ApJS*, 125, 73
- Johnson, R., & Li, W. D. 1999, IAUC No. 7215
- Kogut, A., et al. 1993, *ApJ*, 419, 1
- Krisciunas, K., Hastings, N. C., Loomis, K., McMillan, R., Rest, A., Riess, A. G., & Stubbs, C. 2000, *ApJ*, 539, 658 (Paper I)
- Landolt, A. U. 1992, *AJ*, 104, 340
- Leibundgut, B., Kirshner, R. P., Phillips, M. M., et al. 1993, *AJ*, 105, 301
- Leibundgut, B. 2000, *Astron. Ap. Rev.*, 10, 179
- Lira, P., Suntzeff, N. B., Phillips, M. M., et al. 1998, *AJ*, 115, 234
- Meikle, W. P. S. 2000, *MNRAS*, 314, 782
- Modjaz, M. & Li, W. D. 1999, IAUC No. 7237
- Modjaz, M., Li, W., Filippenko, A. V., King, J. Y., Leonard, D. C., Matheson, T., & Treffers, R. R. 2001, *PASP*, 113, 308
- Nomoto, K., Iwamoto, K., & Kishimoto, N. 1997, *Science*, 276, 1378
- Nugent, P., Phillips, M., Baron, E., Branch, D., & Hauschildt, P. 1995, *ApJ*, 455, L147
- Papenkova, M., & Li, W. D. 1999, IAUC No. 7337
- Perlmutter, S., et al. 1997, *ApJ*, 483, 565
- Persson, S. E., Murphy, D. C., Krzeminski, W., Roth, M., & Rieke, M. J. 1998, *AJ*, 116, 2475

- Phillips, M. M. 1993, *ApJ*, 413, L105
- Phillips, M. M., Lira, P., Suntzeff, N. B., Schommer, R. A., Hamuy, M., & Maza, J. 1999, *AJ*, 118, 1766
- Pinto, P. A., & Eastman, R. G. 2000a, *ApJ*, 530, 744
- Pinto, P. A., & Eastman, R. G. 2000b, *ApJ*, 530, 757
- Puckett, T. 2000, IAUC No. 7417
- Rieke, G. H., & Lebofsky, M. J. 1985, *ApJ*, 288, 618
- Riess, A. G., Press, W. H., & Kirshner, R. P. 1996, *ApJ*, 473, 88 (RPK)
- Riess, A. G., Filippenko, A. V., Challis, P., et al. 1998a, *AJ*, 116, 1009
- Riess, A. G., Nugent, P., Filippenko, A. V., Kirshner, R. P., & Perlmutter, S. 1998b, *ApJ*, 504, 935
- Riess, A. G., Kirshner, R. P., Schmidt, B. P., et al. 1999, *AJ*, 117, 707
- Riess, A. G., Filippenko, A. V., Liu, M. C., et al. 2000, *ApJ*, 536, 62
- Salvo, M. E., Cappellaro, E., Mazzali, P. A., Benetti, S., Danziger, I. J., Patat, F., & Turatto, M. 2001, *MNRAS*, 321, 254
- Schlegel, D. J., Finkbeiner, D. P., & Davis, M. 1998, *ApJ*, 500, 525
- Snedden, C., Gehrz, R. D., Hackwell, J. A., York, D. G., & Snow, T. P. 1978, *ApJ*, 223, 168
- Stetson, P. 1987, *PASP*, 99, 191
- Stetson, P. 1990, *PASP*, 102, 932
- Suntzeff, N. B. 1996, in *Supernovae and Supernova Remnants*, ed. R. McCray & Z. Wang (Cambridge: Cambridge Univ. Press), 41
- Wainscoat, R. J., & Cowie, L. L. 1992, *AJ*, 103, 332

Wheeler, J. C., Höflich, P., Harkness, R. P., & Spyromilio, J. 1998, *ApJ*, 496, 908

Table 1. NGC 6411 Photometric Sequence for SN 1999da

\star	α (2000) ^a	δ (2000) ^a	V	B–V	V–R	V–I
SN	17:35:23.0	+60:48:49				
2	17:35:25.9	+60:47:37	18.311 (0.014)	0.724 (0.022)	0.447 (0.020)	0.842 (0.023)
3	17:35:29.8	+60:47:24	17.861 (0.015)	0.808 (0.016)	0.463 (0.011)	0.852 (0.009)
4	17:35:48.9	+60:48:29	18.171 (0.040)	1.368 (0.120)	1.054 (0.052)	2.360 (0.076)
5	17:35:33.5	+60:50:25	16.904 (0.018)	1.392 (0.015)	0.824 (0.018)	1.590 (0.022)
6	17:35:23.8	+60:52:42	14.656 (0.002)	0.971 (0.006)	0.547 (0.003)	1.075 (0.003)
7	17:35:20.1	+60:50:09	15.121 (0.007)	0.773 (0.004)	0.454 (0.008)	0.838 (0.010)

^aThe field star coordinates were derived from the USNO-A2.0 catalog. Photometry of stars 2, 3, 5, and 7 were calibrated with the Apache Point Observatory 3.5-m telescope on one photometric night. Stars 4 and 6 were calibrated with observations from the Manastash Ridge Observatory 0.76-m telescope.

Table 2. UGC 1087 Photometric Sequence for SN 1999dk

\star	α (2000) ^a	δ (2000) ^a	V	B–V	V–R	V–I
SN	1:31:26.9	+14:17:06				
2	1:31:35.1	+14:14:00	13.555 (0.009)	0.705 (0.016)	0.389 (0.020)	0.747 (0.021)
3	1:31:43.5	+14:15:31	14.374 (0.011)	0.757 (0.012)	0.416 (0.020)	0.785 (0.022)
4	1:31:24.0	+14:18:31	17.207 (0.008)	0.628 (0.017)	0.332 (0.032)	0.665 (0.046)
5	1:31:24.5	+14:19:18	17.294 (0.017)	1.374 (0.054)	0.861 (0.034)	1.625 (0.037)

^aField star coordinates are from the USNO-A2.0 catalog.

Table 3. UGC 1993 Photometric Sequence for SN 1999gp

★	α (2000) ^a	δ (2000) ^a	V	B–V	V–R	V–I
SN	2:31:39.2	+39:22:52				
2	2:31:37.5	+39:23:37	16.823 (0.006)	0.952 (0.009)	0.489 (0.010)	1.042 (0.013)
3	2:31:45.6	+39:22:46	17.410 (0.004)	0.655 (0.007)	0.328 (0.009)	0.778 (0.004)
4	2:31:40.6	+39:21:47	17.986 (0.006)	0.693 (0.005)	0.364 (0.007)	0.807 (0.012)
5	2:31:40.0	+39:21:14	17.265 (0.006)	0.595 (0.016)	0.332 (0.008)	0.776 (0.009)
6	2:31:37.4	+39:21:54	16.862 (0.002)	0.882 (0.007)	0.470 (0.010)	1.018 (0.014)
7	2:31:34.1	+39:21:31	18.309 (0.009)	1.242 (0.005)	0.711 (0.011)	1.456 (0.010)
8	2:31:33.0	+39:23:07	18.959 (0.011)	1.076 (0.016)	0.618 (0.011)	1.315 (0.017)
9	2:31:31.0	+39:24:06	15.821 (0.010)	0.569 (0.006)	0.313 (0.012)	0.758 (0.011)
10	2:31:39.0	+39:21:46	14.499 (0.002)	0.576 (0.008)	0.286 (0.007)	0.655 (0.029)

^aField star coordinates were determined from the USNO-A2.0 catalog.

Table 4. NGC 4520 Photometric Sequence for SN 2000bk

\star	α (2000) ^a	δ (2000) ^a	V	B–V	V–R	V–I
SN	12:33:53.9	–07:22:43				
1	12:33:55.3	–07:22:44	17.882 (0.006)	0.982 (0.013)	0.580 (0.002)	1.086 (0.009)
2	12:33:48.7	–07:23:37	16.462 (0.002)	0.510 (0.009)	0.348 (0.004)	0.690 (0.014)
3	12:33:53.7	–07:23:57	18.282 (0.004)	0.680 (0.012)	0.429 (0.007)	0.860 (0.010)
4	12:33:59.2	–07:23:11	16.192 (0.004)	0.456 (0.007)	0.295 (0.002)	0.582 (0.011)
5	12:34:00.7	–07:21:55	18.340 (0.002)	0.603 (0.011)	0.386 (0.004)	0.748 (0.013)
6	12:33:58.9	–07:21:38	18.095 (0.005)	0.695 (0.014)	0.442 (0.003)	0.854 (0.014)
7	12:33:56.7	–07:20:52	17.744 (0.003)	1.530 (0.016)	0.994 (0.005)	2.054 (0.007)
8	12:33:48.3	–07:22:35	15.000 (0.005)	0.602 (0.012)	0.365 (0.005)	0.719 (0.012)

^aField star coordinates were determined from the USNO-A2.0 catalog.

Table 5. UGC 4195 Photometric Sequence for SN 2000ce

\star	α (2000) ^a	δ (2000) ^a	V	B–V	V–R	V–I
SN	8:05:09.5	+66:47:15				
1	8:05:18.8	+66:47:06	15.725 (0.002)	0.813 (0.005)	0.448 (0.013)	0.870 (0.007)
2	8:05:07.6	+66:46:01	15.829 (0.002)	0.694 (0.004)	0.413 (0.012)	0.821 (0.006)
3	8:05:18.4	+66:45:12	16.815 (0.003)	0.838 (0.022)	0.461 (0.015)	0.893 (0.011)
4	8:05:18.8	+66:46:03	17.342 (0.005)	0.566 (0.006)	0.338 (0.012)	0.691 (0.008)
5	8:05:27.0	+66:46:37	16.043 (0.003)	1.123 (0.005)	0.641 (0.010)	1.192 (0.007)
6	8:05:14.6	+66 47:42	18.337 (0.014)	1.682 (0.089)	1.220 (0.018)	2.759 (0.019)

^aField star coordinates were determined from the USNO-A2.0 catalog.

Table 6. BVRI Photometry of SN 1999da

JD – 2,451,000	Obs ^a	V	B–V	V–R	V–I
366.7340	MRO	16.543 (0.048)	0.810 (0.113)	–0.003 (0.064)	–0.082 (0.068)
367.8058	MRO	16.552 (0.014)	0.480 (0.025)	0.266 (0.017)	0.130 (0.026)
368.7848	MRO	16.462 (0.008)	0.516 (0.015)	0.234 (0.012)	0.161 (0.020)
379.7176	MRO	16.674 (0.012)		0.431 (0.014)	0.599 (0.020)
383.6671	APO	17.163 (0.005)	1.499 (0.006)	0.565 (0.005)	0.912 (0.006)
388.8553	MRO	17.423 (0.032)	1.753 (0.152)	0.364 (0.042)	0.729 (0.041)
392.6838	APO	17.827 (0.026)			0.914 (0.028)
413.6875	MRO	18.800 (0.044)	1.036 (0.132)	0.313 (0.063)	0.714 (0.061)

^aThe MRO data were derived with respect to stars 3, 5, 6 and 7 of the NGC 6411 photometric sequence, while the APO data were derived with respect to stars 3, 5 and 7.

Table 7: BVRI Photometry of SN 1999dk^a

JD – 2,451,000	V	B–V	V–R	V–I
412.9809	14.963 (0.011)		0.006 (0.016)	–0.220 (0.021)
413.8730	14.986 (0.008)	0.082 (0.013)	0.028 (0.014)	–0.229 (0.017)
416.9244	14.923 (0.011)	0.113 (0.019)	–0.002 (0.017)	–0.368 (0.022)
425.8880	15.216 (0.009)	0.497 (0.016)	–0.085 (0.016)	–0.475 (0.025)
426.8637	15.270 (0.008)	0.476 (0.015)	–0.122 (0.016)	–0.458 (0.025)
437.8778	15.820 (0.010)	1.088 (0.024)	0.225 (0.018)	0.256 (0.022)
442.8296	16.136 (0.011)	1.297 (0.026)	0.342 (0.017)	0.438 (0.025)
463.8527	16.966 (0.026)	1.100 (0.059)	0.251 (0.035)	0.317 (0.046)
464.7227	17.053 (0.030)	0.900 (0.050)	0.425 (0.041)	0.309 (0.061)
466.7203	16.998 (0.023)	0.936 (0.045)	0.345 (0.033)	0.393 (0.051)
469.8508	17.154 (0.020)	1.016 (0.044)	0.303 (0.033)	0.289 (0.041)

^aThe data were derived with respect to the four stars of the UGC 1087 photometric sequence.

Table 8: BVRI Photometry of SN 1999gp^a

JD – 2,451,000	V	B–V	V–R	V–I
542.5664	16.626 (0.006)	0.006 (0.005)	0.034 (0.005)	
544.5629	16.424 (0.006)	0.009 (0.004)	0.029 (0.004)	0.019 (0.004)
547.7250	16.224 (0.006)	0.039 (0.004)	–0.011 (0.005)	–0.102 (0.007)
552.5816	16.140 (0.006)	0.146 (0.004)	0.022 (0.003)	–0.278 (0.004)
573.5920	17.020 (0.006)	0.881 (0.004)	0.122 (0.007)	0.103 (0.005)
578.5712	17.199 (0.008)	1.118 (0.005)	0.266 (0.006)	0.366 (0.006)
581.5773	17.326 (0.008)	1.207 (0.004)	0.358 (0.004)	0.534 (0.004)
584.7681	17.467 (0.008)	1.263 (0.007)	0.377 (0.006)	0.680 (0.007)
588.5806	17.709 (0.008)	1.157 (0.014)	0.453 (0.007)	0.766 (0.011)
601.5890	18.242 (0.008)	0.973 (0.011)	0.321 (0.008)	0.598 (0.010)
614.5984	18.588 (0.008)	0.938 (0.009)	0.283 (0.009)	0.370 (0.016)
616.5987	18.642 (0.010)	1.075 (0.041)		0.527 (0.024)
630.6122	18.950 (0.008)	0.721 (0.012)	0.177 (0.009)	0.254 (0.015)

^aThe data were derived with respect to stars 2, 3, 6, 9, and 10 of the UGC 1993 photometric sequence.

Table 9: BVRI Photometry of SN 2000bk^a

JD – 2,451,000	V	B–V	V–R	V–I
658.6877	17.289 (0.003)	0.746 (0.006)	0.086 (0.004)	–0.071 (0.008)
660.6091	17.431 (0.007)	0.859 (0.015)	0.123 (0.009)	–0.029 (0.014)
665.8727	17.832 (0.005)	1.252 (0.013)	0.371 (0.006)	0.473 (0.012)
672.6898	18.425 (0.003)	1.273 (0.009)	0.559 (0.004)	0.898 (0.007)
675.6409	18.672 (0.005)	1.206 (0.012)	0.526 (0.006)	0.867 (0.008)
684.6444	19.061 (0.006)	1.229 (0.016)	0.405 (0.008)	0.631 (0.011)
686.6370	19.164 (0.006)	1.192 (0.020)	0.427 (0.008)	0.642 (0.013)
689.6738	19.261 (0.005)	1.126 (0.010)	0.398 (0.007)	0.584 (0.011)
693.6645	19.401 (0.005)	1.113 (0.012)	0.306 (0.007)	0.521 (0.014)

^aThe data were derived with respect to stars 1, 2, 4, 7, and 8 of the NGC 4520 photometric sequence.

Table 10: BVRI Photometry of SN 2000ce^a

JD – 2,451,000	V	B–V	V–R	V–I
675.6212	16.864 (0.005)	0.778 (0.012)	0.297 (0.009)	0.272 (0.007)
684.6168	17.442 (0.018)	1.081 (0.036)	0.392 (0.022)	0.638 (0.023)
686.6237	17.467 (0.011)	1.259 (0.043)	0.338 (0.015)	0.699 (0.015)
689.6343	17.616 (0.004)	1.489 (0.010)	0.492 (0.008)	0.900 (0.007)
693.6401	17.796 (0.005)	1.640 (0.017)	0.601 (0.009)	1.117 (0.008)
707.6451	18.515 (0.015)	1.665 (0.065)	0.682 (0.021)	1.316 (0.021)
711.6397	18.671 (0.017)	1.825 (0.071)	0.636 (0.021)	1.271 (0.020)

^aThe data were derived with respect to stars 1, 2, 4, and 5 of the UGC 4195 photometric sequence.

Table 11: Infrared Magnitudes of Field Stars

Field	Star	J	H	K'	N _{obs} (J,H,K)
SN 1999gp ^a	6	15.16(0.02)	14.68(0.02)	14.56(0.02)	2,1,2
	10	13.34(0.02)	13.08(0.02)	13.03(0.02)	2,1,2
SN 2000bk	1	16.130(0.010)	15.602(0.012)		7,7,0
	2	15.357(0.013)	14.995(0.013)		7,7,0
	8	13.802(0.007)	13.448(0.010)		7,7,0
SN 2000ce	1	14.220(0.024)	13.830(0.020)	13.800(0.026)	3,5,4
	2	14.468(0.030)	14.069(0.023)	14.109(0.028)	2,4,3
	6	14.136(0.024)	13.531(0.020)	13.338(0.025)	3,5,4

^a Preliminarily 2MASS values for star 6 are $J = 15.13 \pm 0.05$, $H = 14.62 \pm 0.06$, $K_s = 14.53 \pm 0.10$. For star 10 2MASS gives $J = 13.35 \pm 0.02$, $H = 13.10 \pm 0.03$, and $K_s = 13.08 \pm 0.06$. (See <http://irsa.ipac.caltech.edu>.)

Table 12. Infrared Photometry of SNe 1999gp, 2000bk and 2000ce

SN	JD– 2,451,000	Obs ^a	J ^b	H	K'	K ^c
1999gp	539.57	APO	17.31 (0.06)		17.74 (0.25)	
	561.66	APO		17.40 (0.13)	16.71 (0.11)	16.51 (0.15)
	564.82	APO	18.67 (0.19)	17.45 (0.14)	17.27 (0.18)	17.22 (0.23)
	568.79	APO	18.29 (0.12)	17.16 (0.11)	17.18 (0.17)	17.19 (0.22)
2000bk	653.77	LCO1	17.64 (0.02)	17.60 (0.04)		
	654.73	LCO1	17.81 (0.03)	17.68 (0.04)		
	658.67	LCO2	18.38 (0.03)	17.74 (0.03)		
	659.63	LCO2	18.41 (0.03)	17.65 (0.03)		
	660.59	LCO2	18.36 (0.03)	17.61 (0.03)		
	660.75	APO	18.28 (0.12)	17.50 (0.07)		
	661.73	LCO1	18.66 (0.04)	17.73 (0.05)		
	662.68	LCO1	18.45 (0.04)	17.63 (0.05)		
	663.63	LCO1	18.50 (0.05)	17.58 (0.05)		
	664.59	LCO1	18.53 (0.04)			
	665.65	LCO1	18.48 (0.05)	17.65 (0.05)		
	665.84	APO		17.50 (0.06)		
	666.65	LCO1	18.27 (0.04)	17.58 (0.04)		
	667.60	LCO1	18.22 (0.04)	17.45 (0.05)		
	672.76	APO	17.85 (0.08)			
	676.61	LCO2	18.39 (0.02)	17.94 (0.04)		
	681.65	LCO2	18.92 (0.04)	18.15 (0.05)		
	683.57	LCO2	19.08 (0.04)	18.20 (0.05)		

Table 12—Continued

SN	JD– 2,451,000	Obs ^a	J ^b	H	K'	K ^c
	686.51	LCO2	19.35 (0.08)			
2000ce	675.75	APO	16.82 (0.03)	16.46 (0.03)	16.16 (0.04)	16.08 (0.05)
	684.72	APO	17.57 (0.04)	16.42 (0.03)	16.13 (0.04)	16.04 (0.05)
	686.71	APO	17.44 (0.04)	16.25 (0.03)	16.05 (0.04)	16.00 (0.05)
	689.77	APO		16.32 (0.03)	16.11 (0.07)	16.20 (0.07)
	693.74	APO		16.12 (0.03)	16.01 (0.04)	15.98 (0.05)

^aAPO = Apache Point Observatory 3.5-m; LCO1 = Las Campanas 1-m; LCO2 = Las Campanas 2.5-m. ^bThe LCO observations were made with a J_s filter. ^cUsing the transformation of Wainscoat & Cowie (1992), $K = 1.282 K' - 0.282 H$.

Table 13: MLCS Parameters for Type Ia Supernovae^a

Object	T(B _{max})	Δ	A _V	m–M	D (Mpc)	V _{CMB} (km s ^{–1})
SN 1999dk	414.30 (0.40)	–0.38 (0.08)	0.20 (0.16)	34.45 (0.18)	77.6 ^{+6.7} _{–6.2}	4218
SN 1999gp	551.1 (0.2)	–0.45 (0.10)	0.30 (0.19)	35.67 (0.19)	136.1 ^{+9.8} _{–9.0}	7770
SN 2000bk	648.5 (1.0)	+0.43 (0.15)	0.28 (0.20)	35.53 (0.21)	127.6 ^{+13.0} _{–11.7}	7995
SN 2000ce	666.3 (1.0)	–0.26 (0.17)	1.67 (0.20)	34.69 (0.22)	86.7 ^{+9.2} _{–8.4}	5088

^aB-band maximum is given as Julian Date *minus* 2,451,000.

Δ the number of magnitudes that the object is brighter than (negative values) or fainter than (positive values) the fiducial Type Ia SN.

A_V is the total V-band extinction (due to our Galaxy *and* due to the host galaxy).

m–M = 5 log *d* – 5 is the distance modulus in magnitudes, where *d* is in pc.

D is the distance in megaparsecs.

The radial velocities (V_{CMB}) have been corrected for the motion of the Galaxy toward the Local Group and the motion of the Local Group with respect to the Cosmic Microwave Background Radiation (Kogut et al. 1993).

Table 14: Light Curve Solutions Following Phillips et al. (1999)^a

Object	T(B _{max})	Δ m ₁₅ (B)	B _{max}	V _{max}	I _{max}	E(B–V) _{host}	m–M
SN 1999da	370.3(0.6)	1.94(10)	16.84(06)	16.11(06)	15.85(04)	0.00(05)	
SN 1999dk	414.5(0.2)	1.00(10)	15.06(05)	14.91(05)	15.22(05)	0.07(03)	34.24(09)
SN 1999gp	552.2(0.1)	1.00(10)	16.23(05)	16.11(05)	16.34(05)	0.07(03)	35.40(09)
SN 2000bk	647.9(0.2)	1.63(10)	16.98(20)	16.81(15)	16.81(15)	0.10(04)	35.48(23)
SN 2000ce	665.7(2.3)	0.99(10)	17.24(20)	16.63(16)	16.12(19)	0.54(04)	34.32(14)

^aThe values in parentheses and without a decimal point are uncertainties in hundredths of a magnitude.

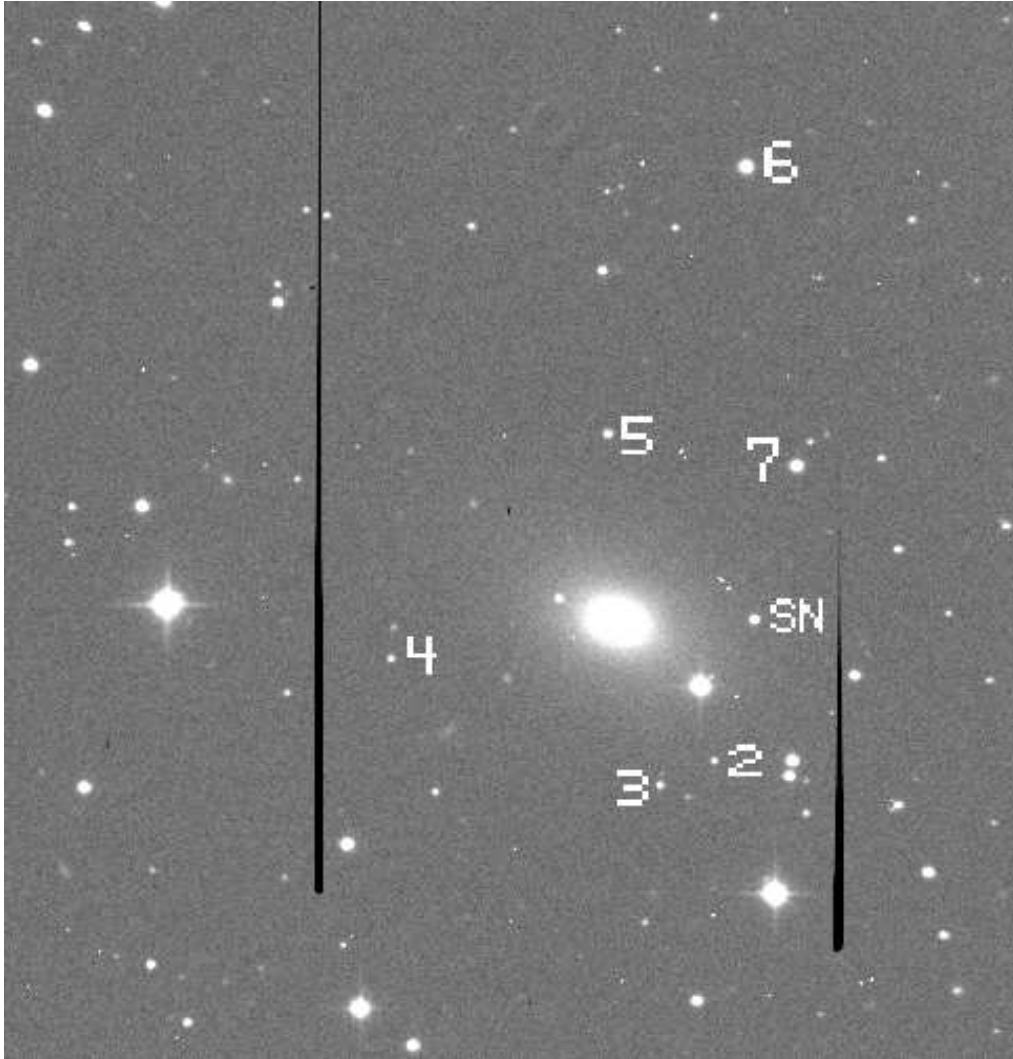


Fig. 1.— A V-band image of NGC 6411 obtained at MRO on 9 July 1999, with SN 1999da and the stars of the photometric sequence indicated. The field is 11 arcmin on a side. North is up, east to the left.

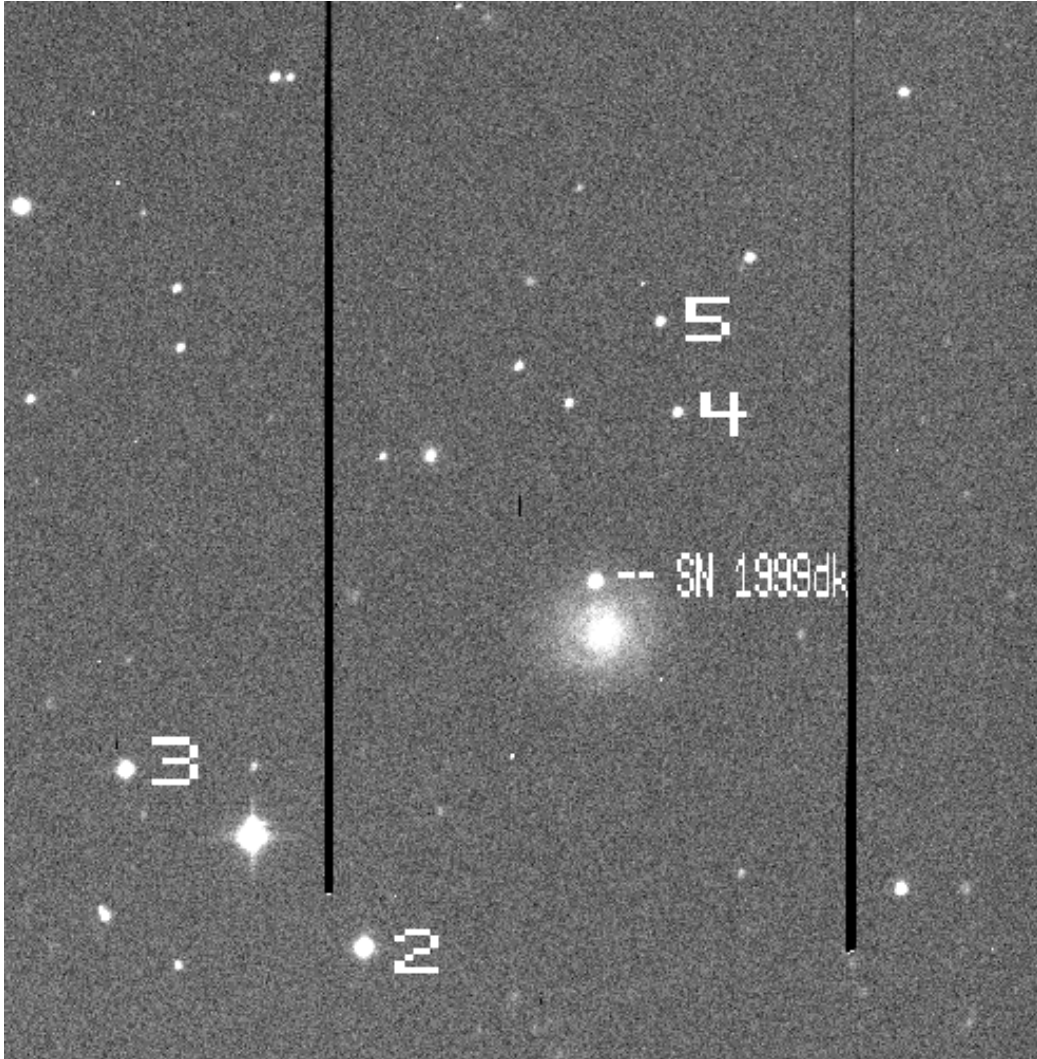


Fig. 2.— A V-band image of UGC 1087 obtained at MRO on 23 August 1999, with SN 1999dk and the stars of the photometric sequence indicated. The field is 11 arcmin on a side. North is up, east to the left.

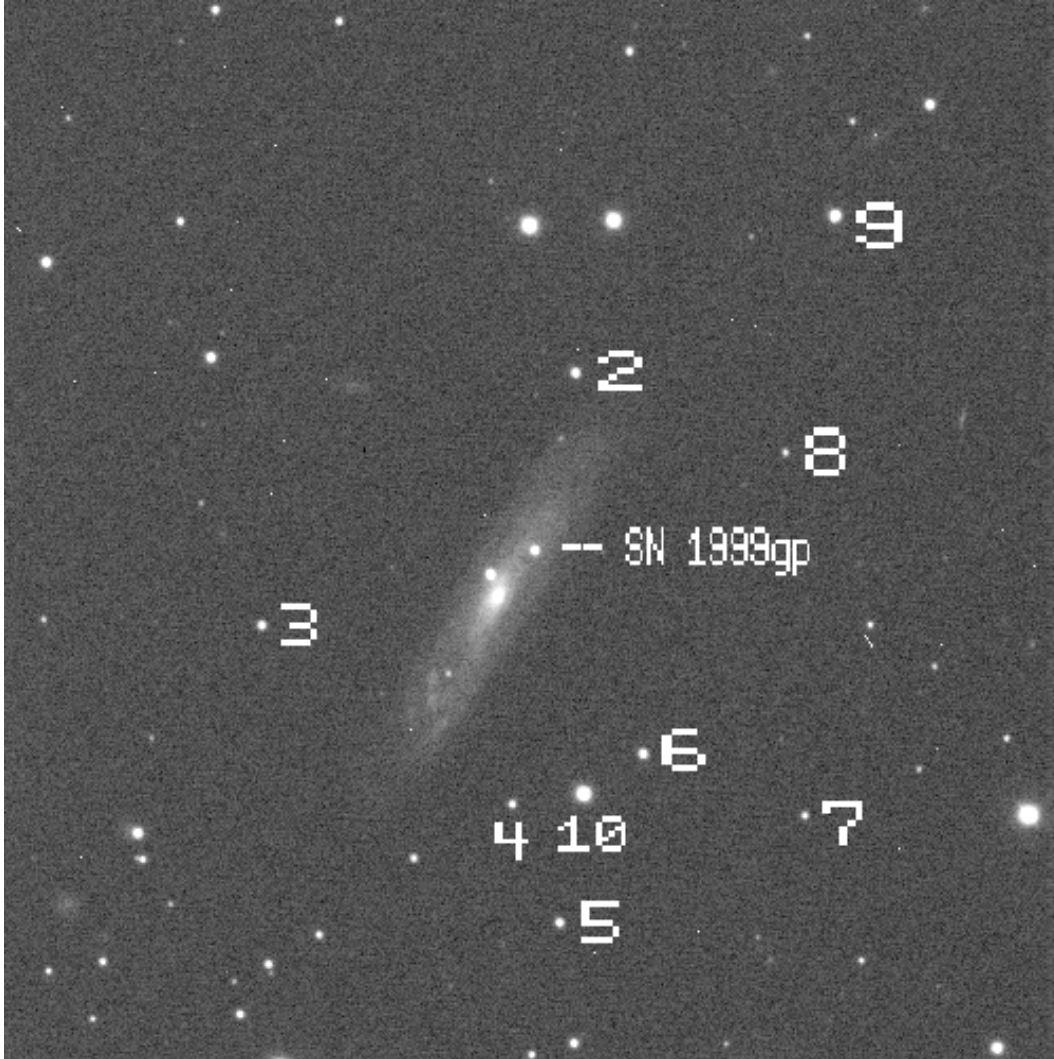


Fig. 3.— A V-band image of UGC 1993 taken on 30 December 1999, with SN 1999gp and the stars of the photometric sequence indicated. The field is 4.8 arcmin on a side. The image is rotated 10 degrees counterclockwise from north up, east to the left.

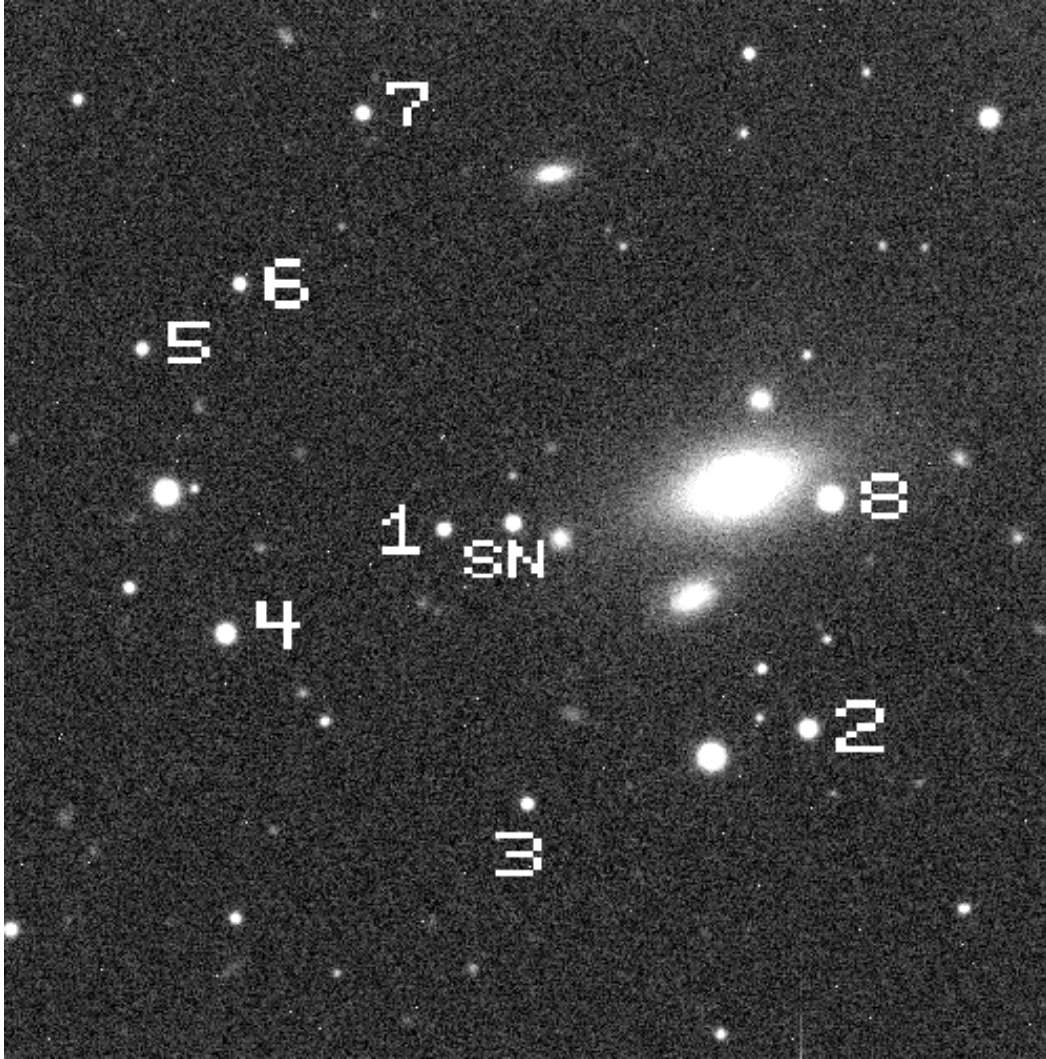


Fig. 4.— A V-band image of NGC 4520 taken on 24 April 2000, with SN 2000bk and the stars of the photometric sequence indicated. The field is 4.8 arcmin on a side. North is up, east to the left.

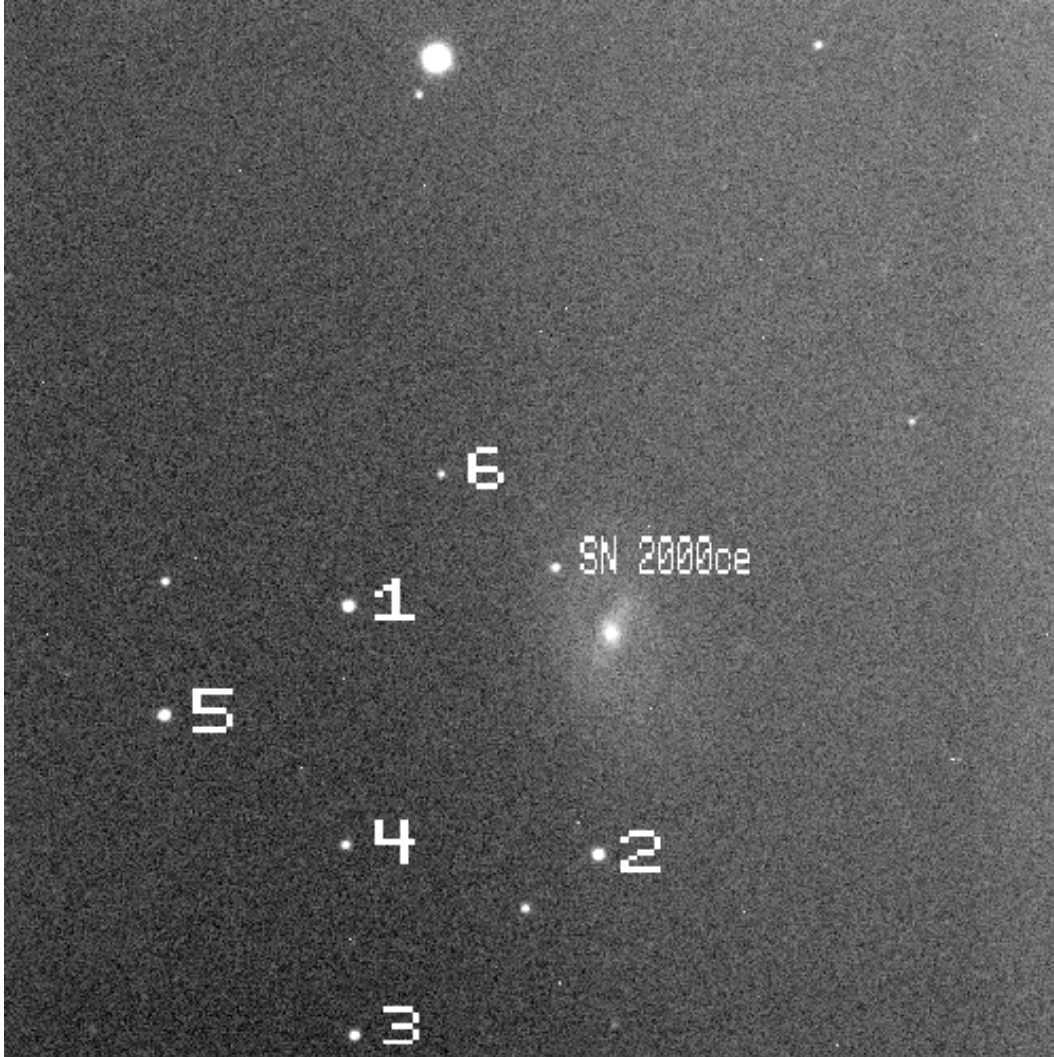


Fig. 5.— A V-band image of UGC 4195 taken on 22 May 2000, with SN 2000ce and the stars of the photometric sequence indicated. The field is 4.8 arcmin on a side. North is up, east to the left.

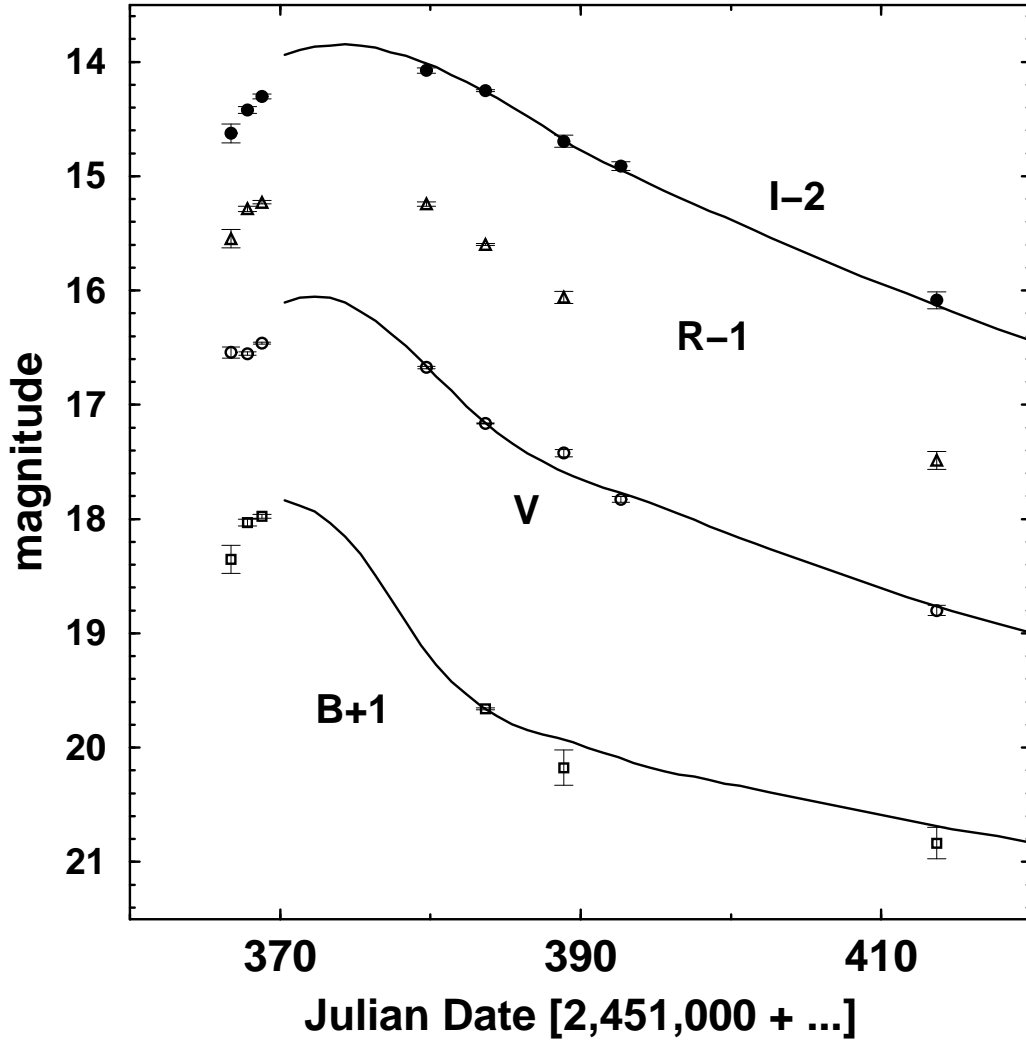


Fig. 6.— BVRI photometry of SN 1999da. The B, R, and I data have been offset vertically by +1, -1, and -2, magnitudes, respectively. The BVI fits are based on templates from the $\Delta m_{15}(B)$ method of Phillips et al. (1999).

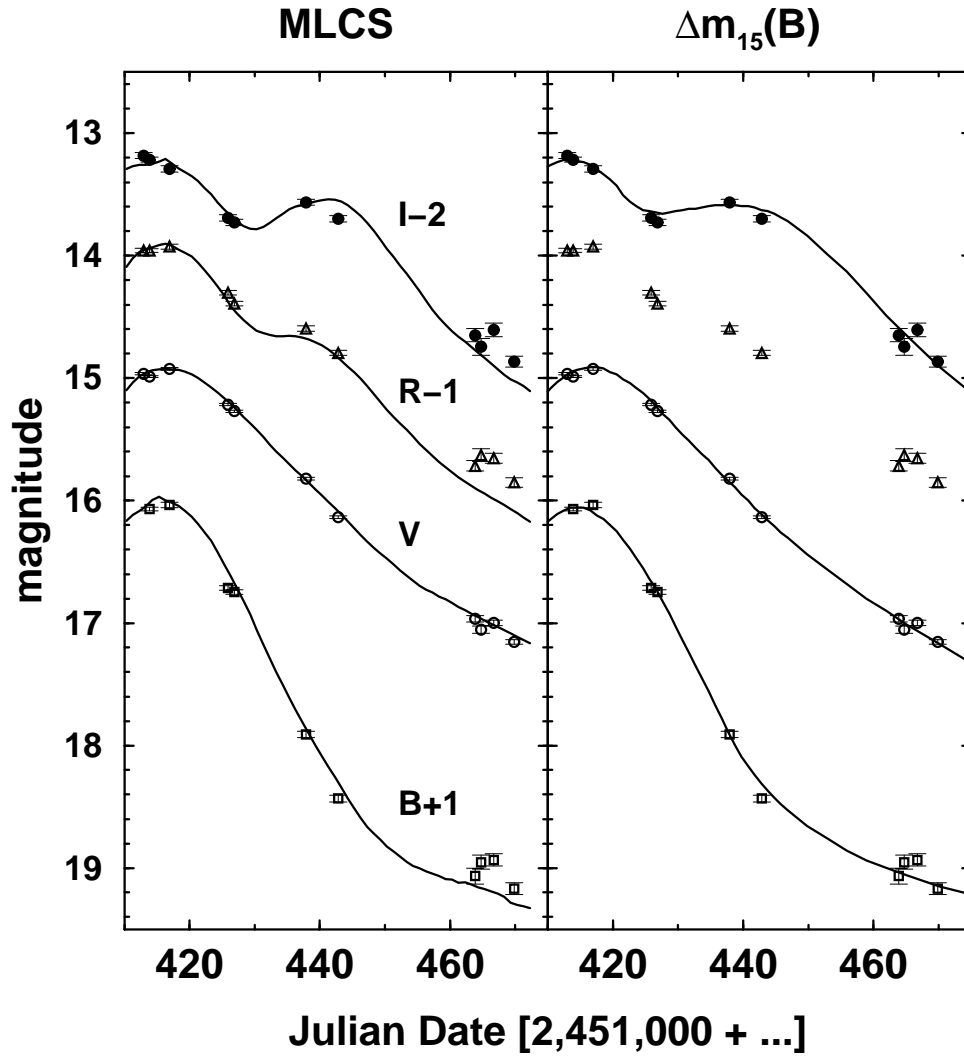


Fig. 7.— BVRI photometry of SN 1999dk. The B, R, and I data have been offset vertically by +1, -1, and -2, magnitudes, respectively. The solid lines in the left hand panel are based on MLCS v/2.0 empirical fits with $\Delta = -0.38$ mag. The BVI fits in the right hand panel are based on templates from the $\Delta m_{15}(B)$ method of Phillips et al. (1999).

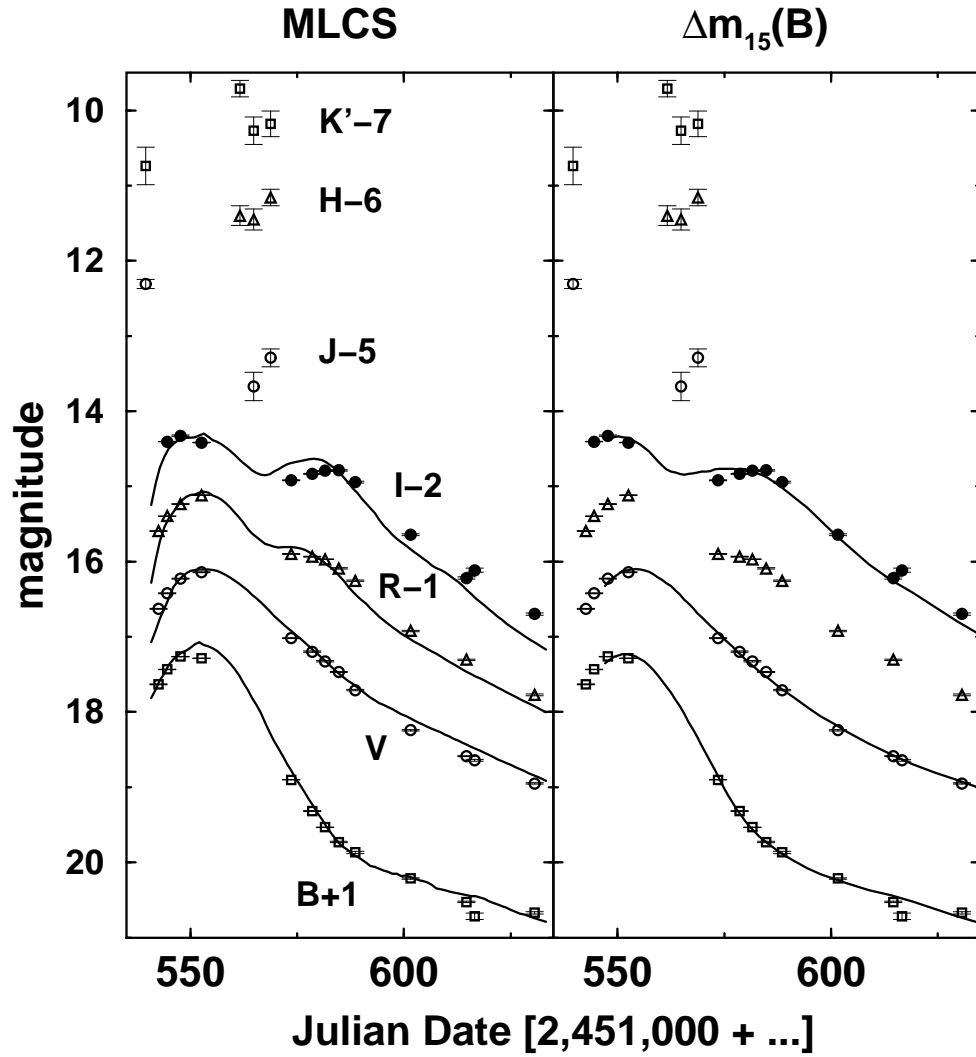


Fig. 8.— BVRI photometry of SN 1999gp. The B, R, I, J, H, and K' data have been offset vertically by +1, -1, -2, -5, -6, and -7 magnitudes, respectively. MLCS v/2.0 templates with $\Delta = -0.45$ are shown in the left hand panel. The BVI fits in the right hand panel are based on templates from the $\Delta m_{15}(B)$ method of Phillips et al. (1999).

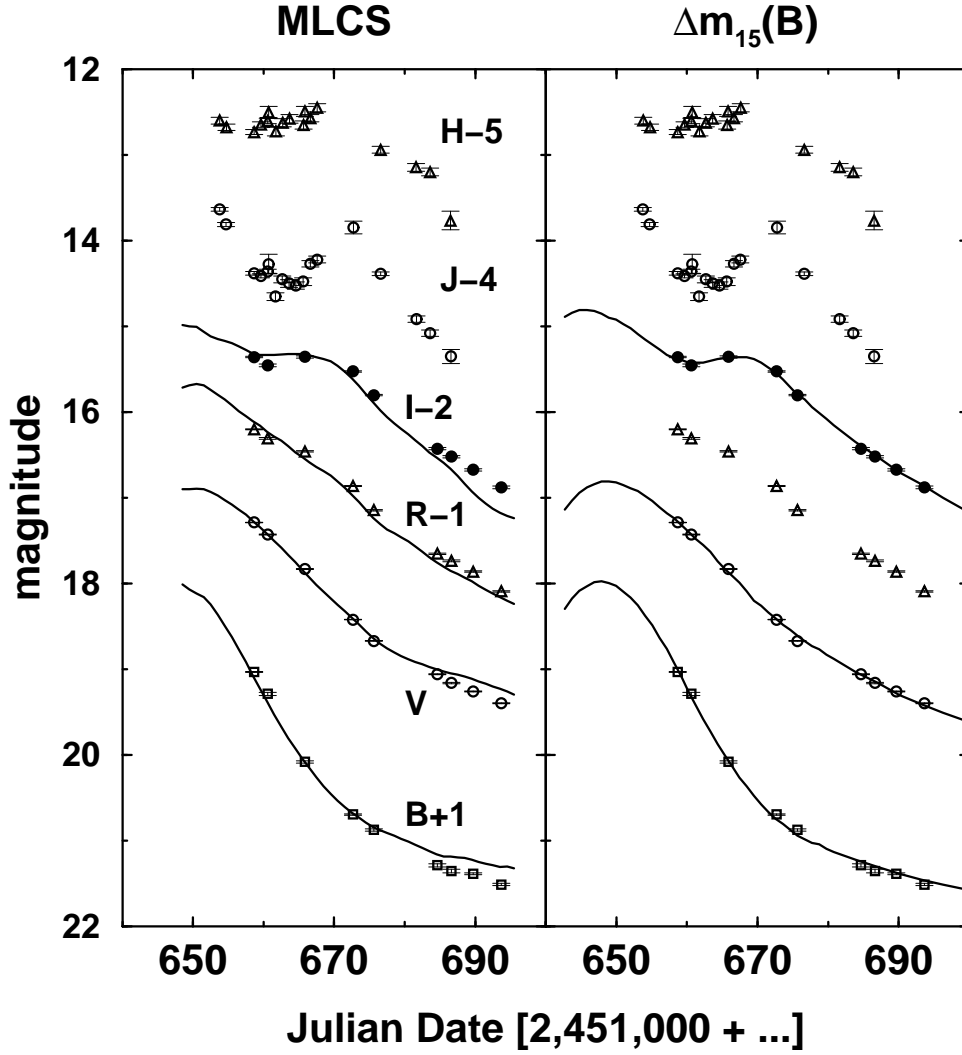


Fig. 9.— BVRI and near infrared photometry of SN 2000bk, with MLCS v/2.0 fits using $\Delta = +0.43$ shown in the left hand panel. The BVI fits in the right hand panel are based on templates from the $\Delta m_{15}(B)$ method of Phillips et al. (1999). The B, R, I, J, and H data have been offset vertically by +1, -1, -2, -4, and -5 magnitudes, respectively. Most of the J-band photometry was actually obtained with a J_s filter.

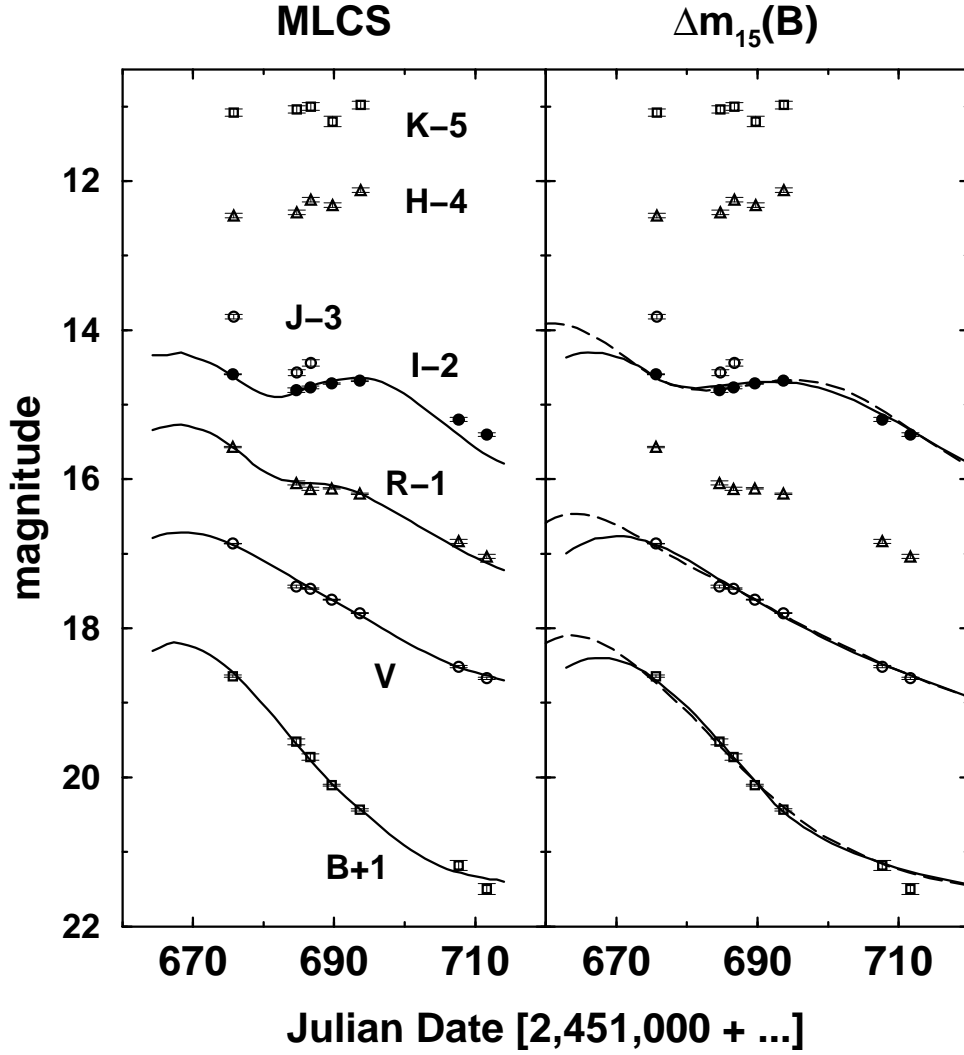


Fig. 10.— BVRI photometry of SN 2000ce, with MLCS v/2.0 fits using $\Delta = -0.26$ shown in the left hand panel. Two templates from the $\Delta m_{15}(B)$ method of Phillips et al. (1999) are shown in the right hand panel and fit the data equally well. This implies a greater than normal uncertainty in the time of maximum light and the magnitudes at maximum. The B, R, I, J, H, and K data have been offset vertically by +1, -1, -2, -3, -4, and -5 magnitudes, respectively.

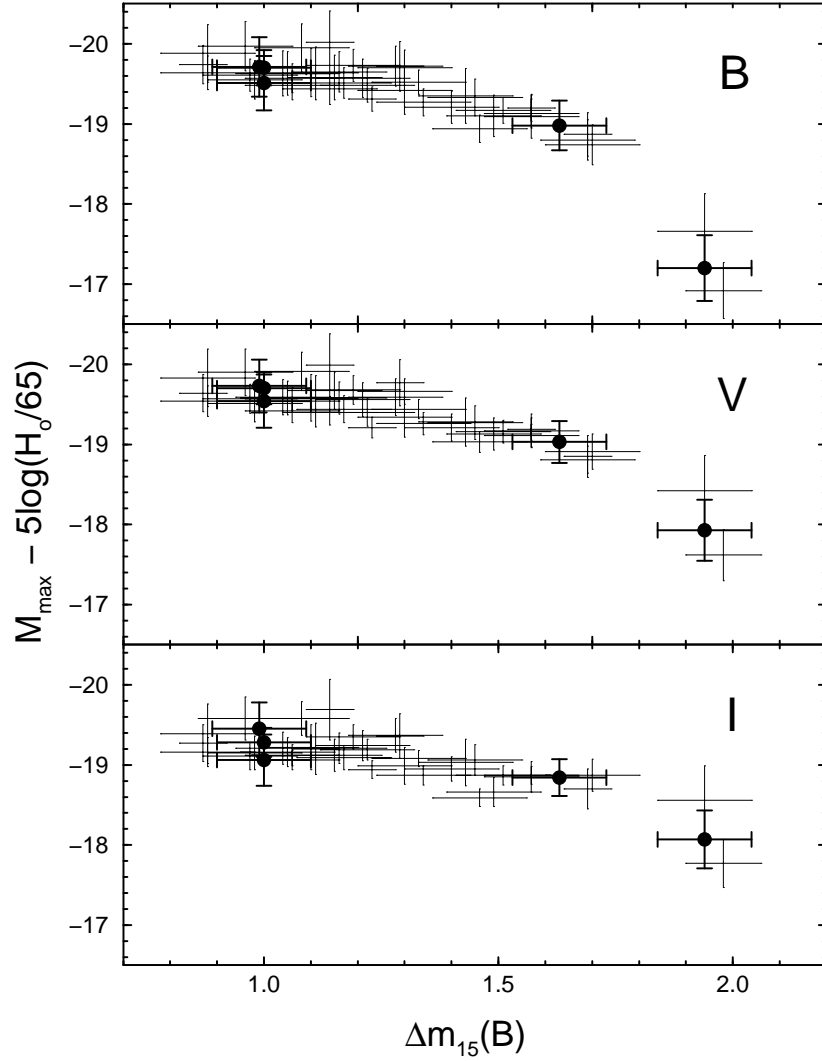


Fig. 11.— Absolute magnitudes at maximum for the 5 SNe from this paper (filled symbols), plus 41 SNe from Phillips et al. (1999), and SN 1998de (Modjaz et al. 2001). All of these objects have redshift $z \gtrsim 0.01$, so the effect of peculiar motions should not significantly contribute to the scatter.

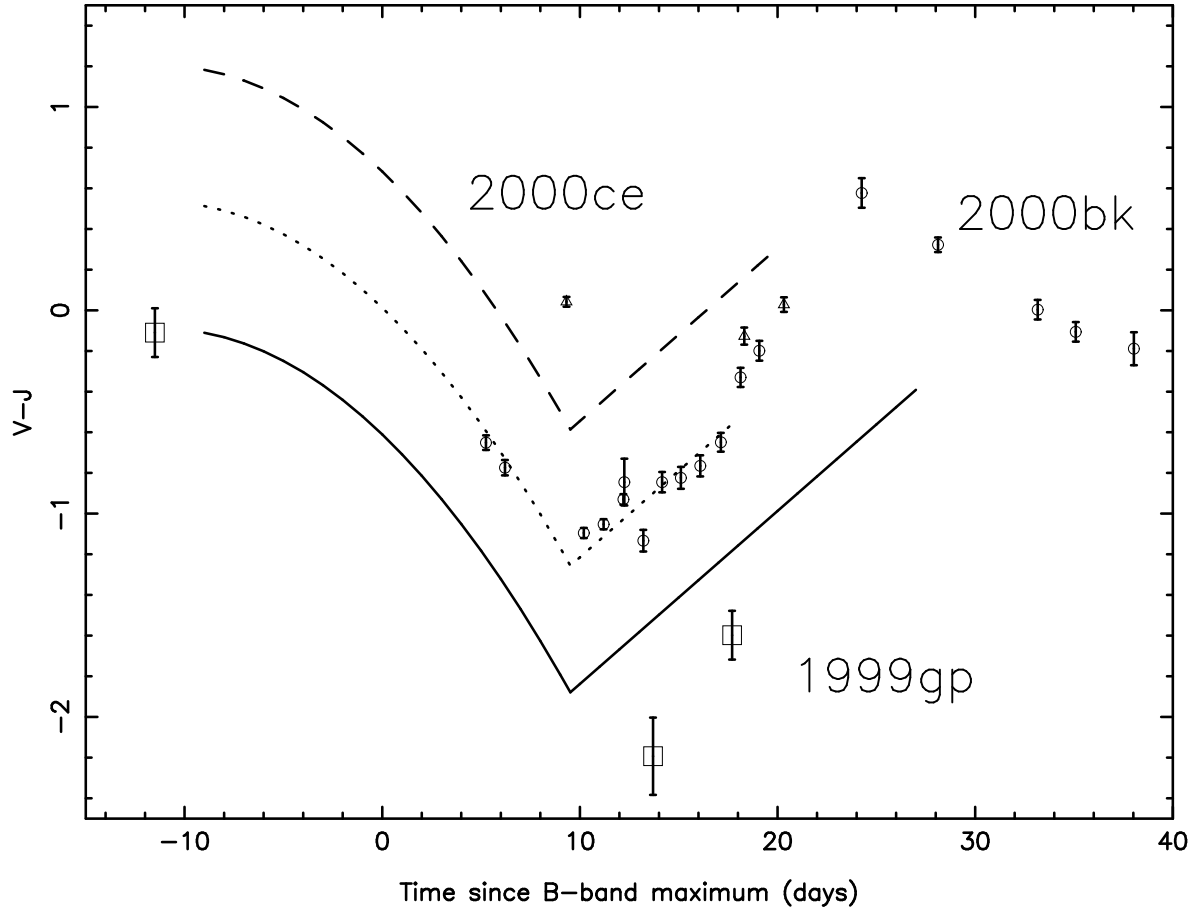


Fig. 12.— Observed $V-J$ colors of SNe 1999gp (squares), 2000bk (open circles), and 2000ce (triangles). The solid line is the $V-J$ unreddened locus from Table 9 of Krisciunas et al. (2000). The dotted line is the unreddened locus offset by 0.62 mag. Clearly, a simple upward translation of the unreddened locus does not fit the shape of the $V-J$ color curve for SN 2000bk beyond $t = 18$ days. The dashed line is the unreddened locus offset by 1.29 mag; it only fits the SN 2000ce points well if the points are shifted 3.0 days to the left.

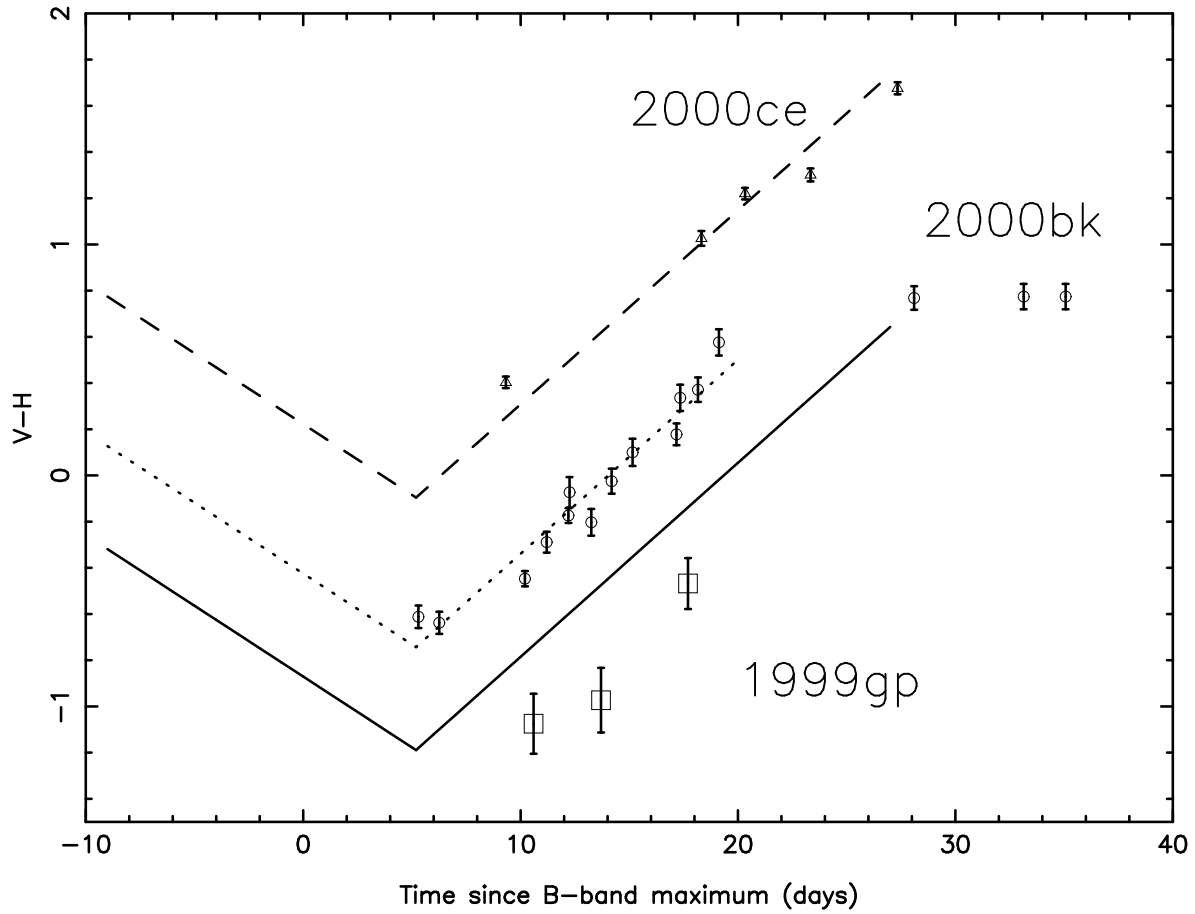


Fig. 13.— Observed $V-H$ colors of SNe 1999gp, 2000bk, and 2000ce. The solid line is the $V-H$ unreddened locus from Table 9 of Krisciunas et al. (2000). The dotted line is the unreddened locus offset by 0.45 mag. The dashed line is the unreddened locus offset by 1.09 mag.

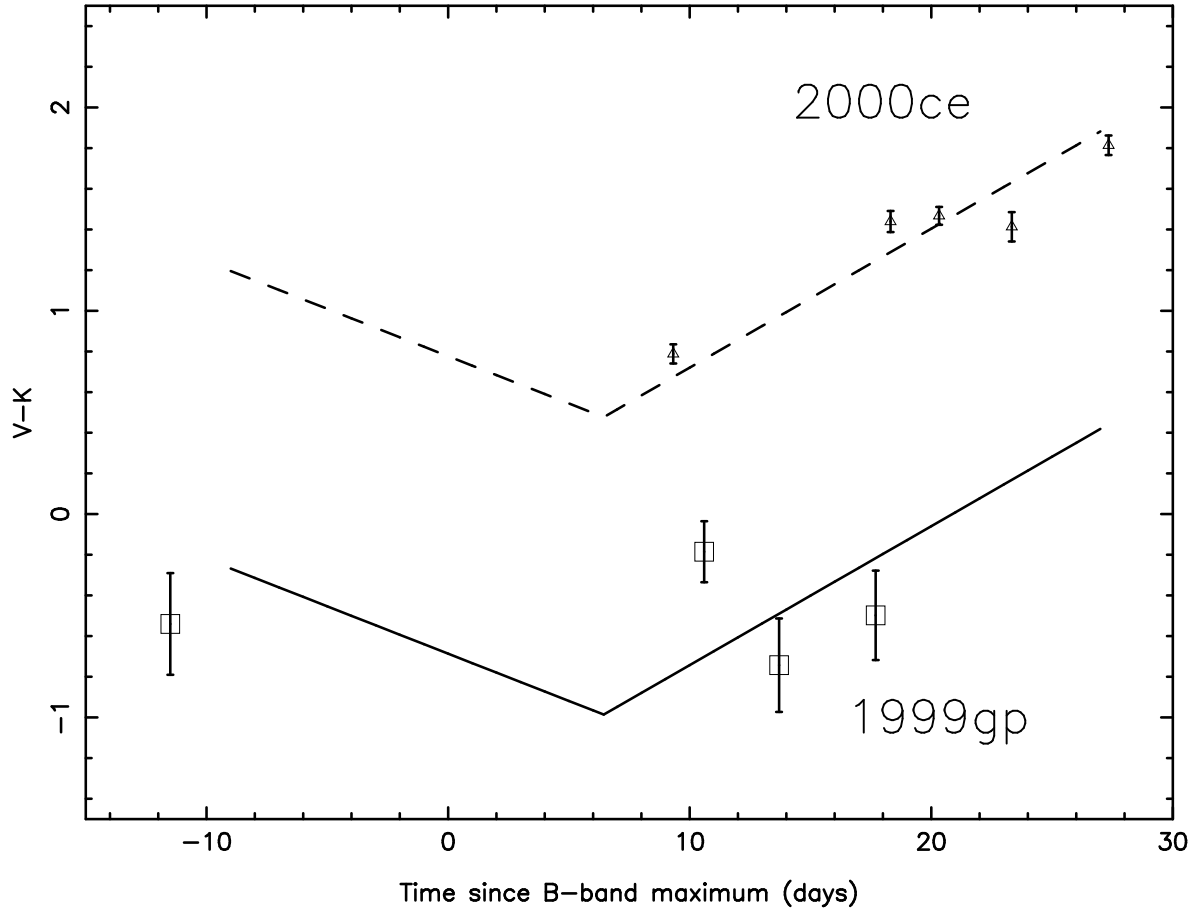


Fig. 14.— Observed $V-K$ colors of SNe 1999gp and 2000ce. The solid line is the $V-K$ unreddened locus from Table 9 of Krisciunas et al. (2000). The dashed line is the unreddened locus offset by 1.46 mag. The leftmost point for SN 1999gp is actually $V-K'$.

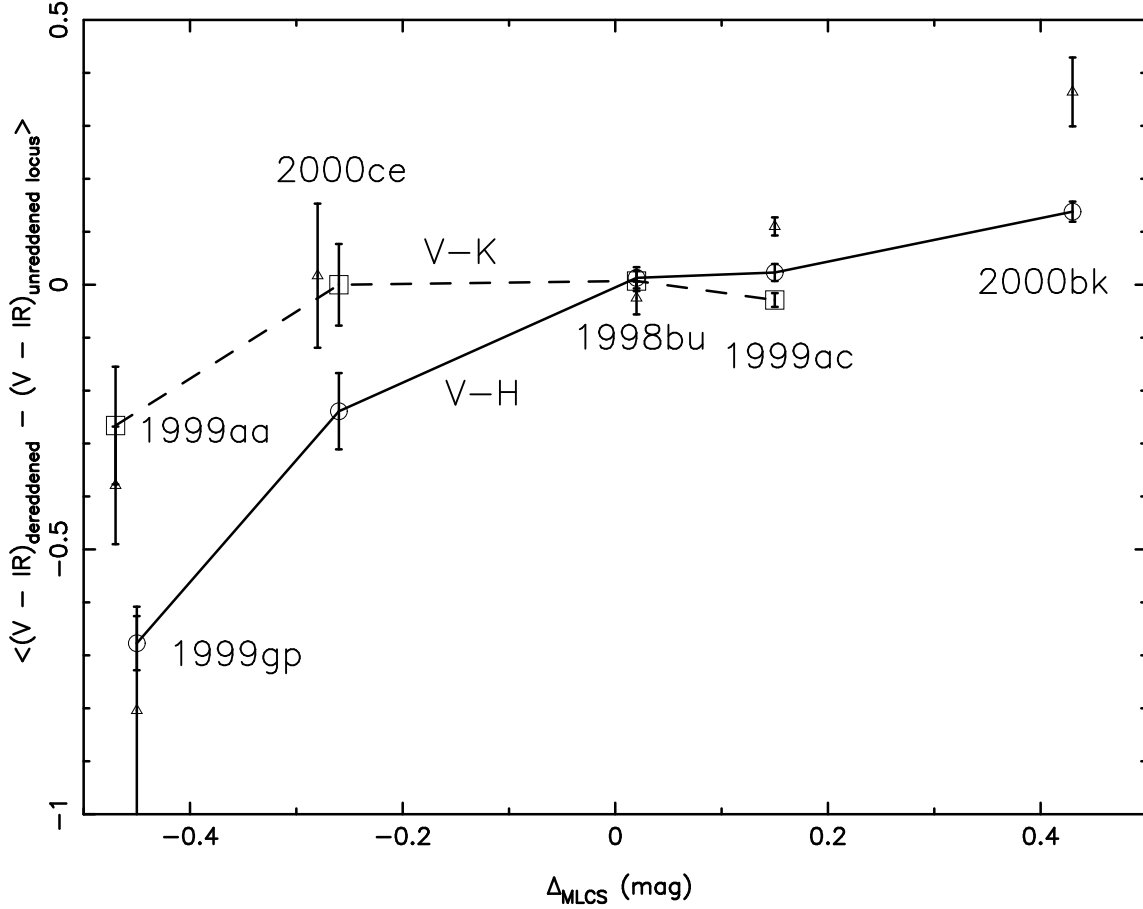


Fig. 15.— We have dereddened the V–J (triangles), V–H (circles) and V–K (squares) colors for several supernovae and determined the mean residuals of those data with respect to unreddened loci derived from data used for Paper I. Except for SN 1998bu we have restricted the data to $0 \leq t \leq 27$ days after the time of B-band maximum. We have horizontally offset the J-band point for SN 2000ce for plotting purposes. The solid line and dashed line are naive connect-the-dots “fits” to the V–H and V–K data, respectively. This figure shows that the mean residual is near zero for V–K over a range of luminosity-at-maximum. Overluminous, slowly declining supernovae like 1999aa and 1999gp are intrinsically bluer in V– near IR color indices than more rapidly declining objects. More rapidly declining objects like SN 2000bk have redder colors than the mid-range decliners.

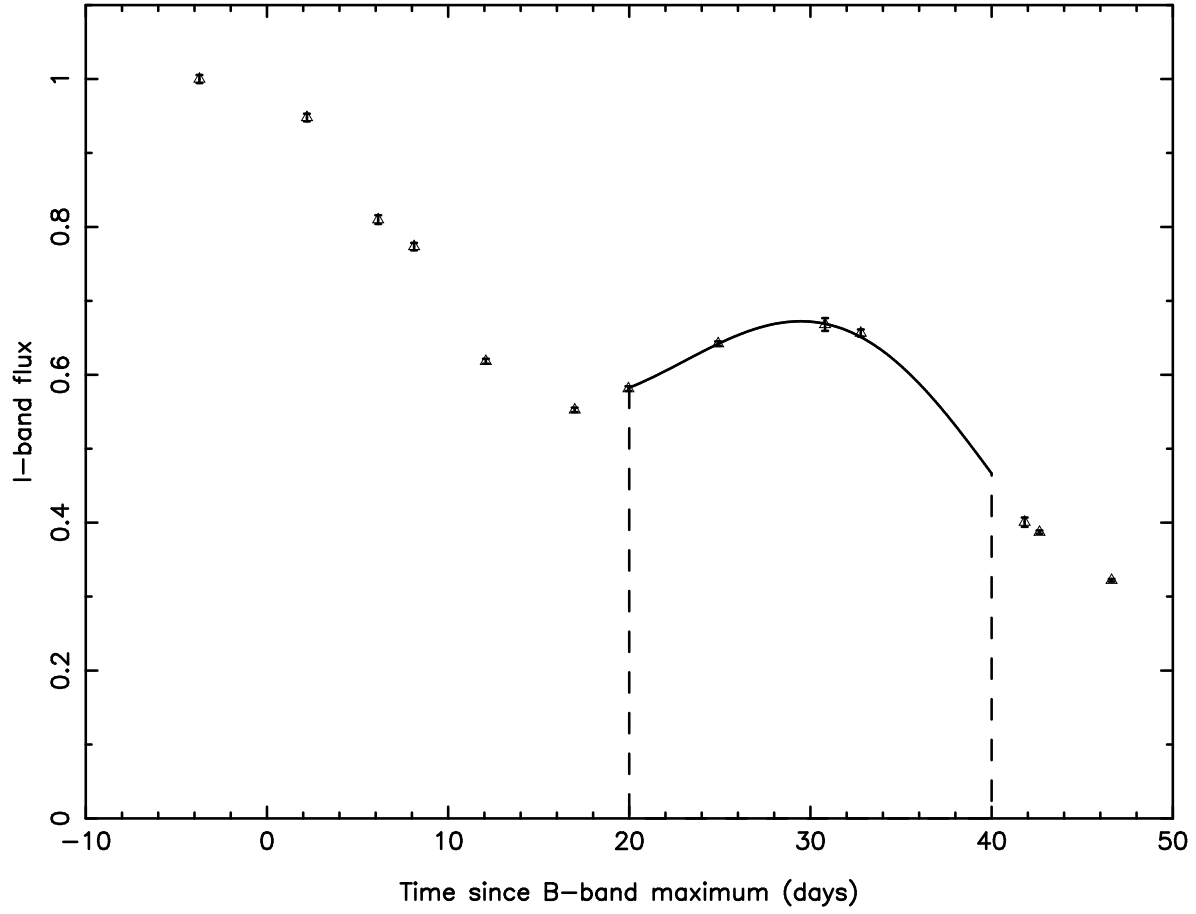


Fig. 16.— I-band light curve of SN 1999aa, with the magnitudes converted to flux units and normalized to the maximum brightness. An integration of a polynomial fit to the data allows us to determine the mean flux from 20 to 40 days after the time of B-band maximum, $\langle I \rangle_{20-40}$.

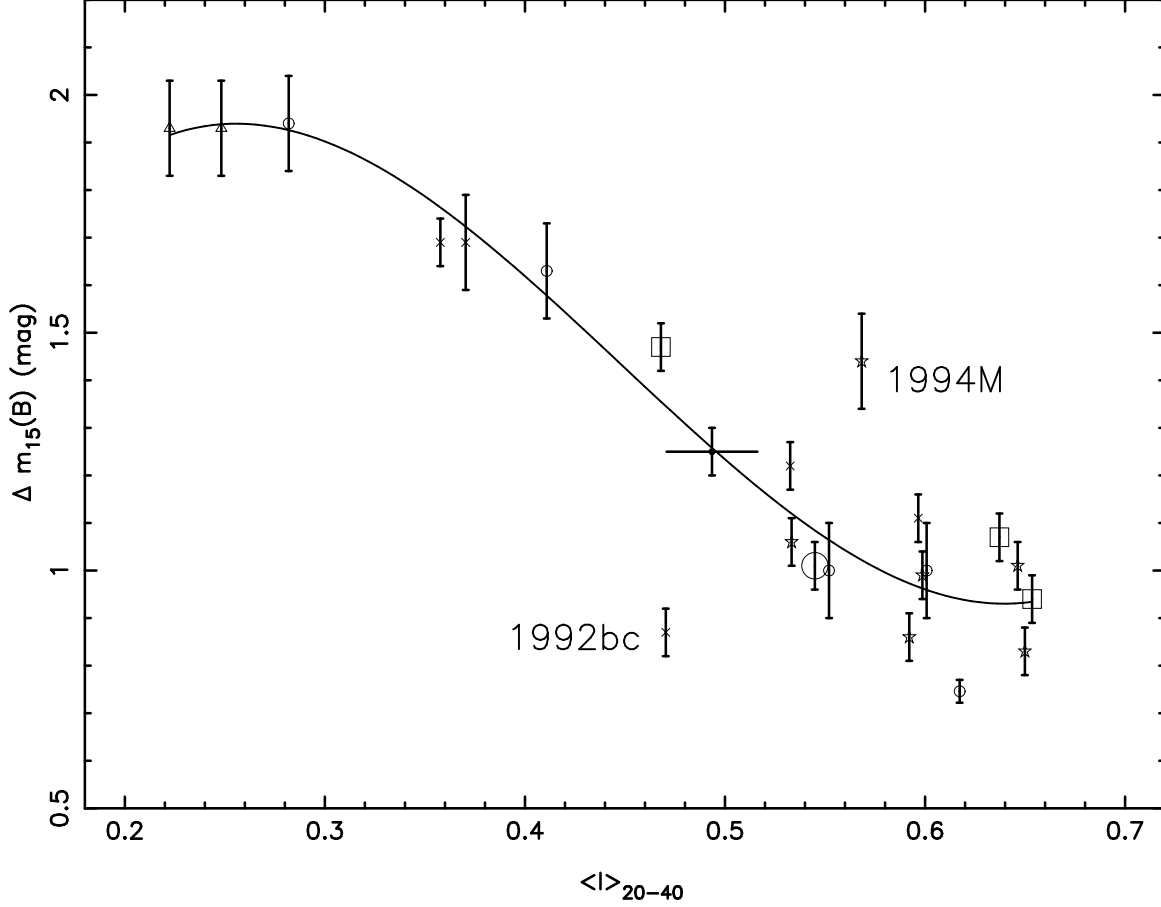


Fig. 17.— The decline rate parameter $\Delta m_{15}(B)$ vs. the mean I-band flux 20 to 40 days after the time of B-band maximum. Symbols: squares – three SNe from the RPK training set; triangles – SNe 1992K and 1991bg; large open circle – SN 1998bu; X's – five SNe from the Calán/Tololo survey; five pointed stars – six SNe from Riess et al. (1999); small open circles – four SNe from this paper, plus SN 1999aa (Paper I); the point with the horizontal error bar represents the mean of the values derived from the SN 1996X data sets of Riess et al. (1999) and R. Covarrubias et al. (unpublished). The two objects which are found furthest from the third order regression line are labeled.

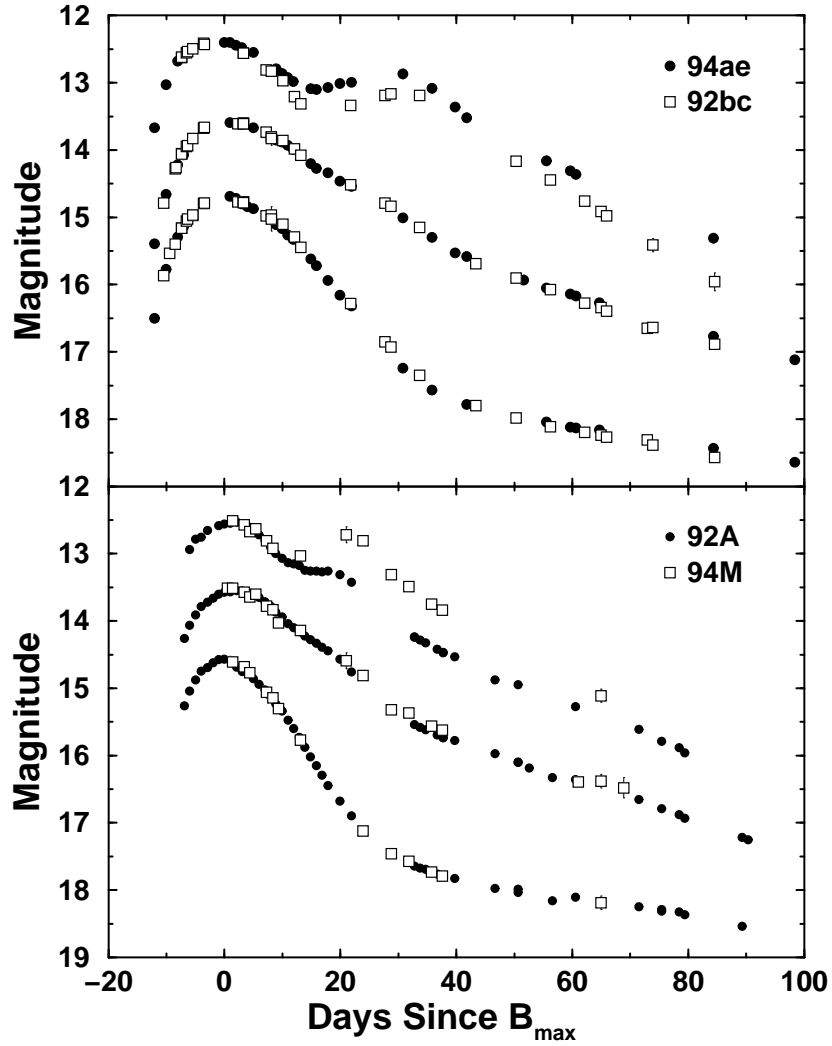


Fig. 18.— In each panel we show, from the top down, the I-, V-, and B-band light curves of Type Ia supernovae, with the photometry adjusted to make the maxima coincide. These two pair of supernovae illustrate that objects can have identical decline rates in B and V, yet have greatly different I-band secondary maxima.